

# Plasmid stability in fluctuating environments: population genetics of multi-copy plasmids

J. Carlos R. Hernandez-Beltran<sup>1</sup>, Verónica Miró Pina<sup>2</sup>, Arno Siri-Jegousse<sup>3</sup>, Sandra Palau<sup>3</sup>, Rafael Peña-Miller<sup>1</sup>, and Adrian Gonzalez Casanova<sup>4</sup>

<sup>1</sup>UNAM CCG

<sup>2</sup>Center for Genomic Regulation

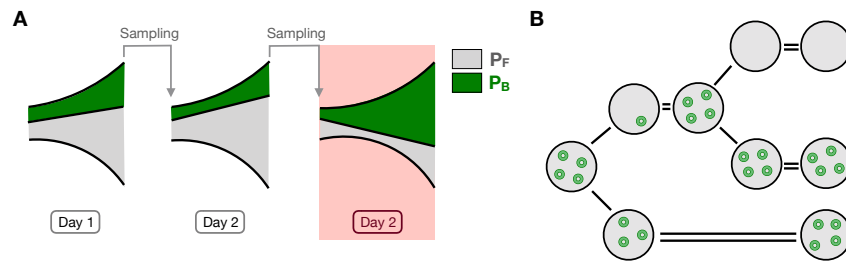
<sup>3</sup>UNAM IIMAS

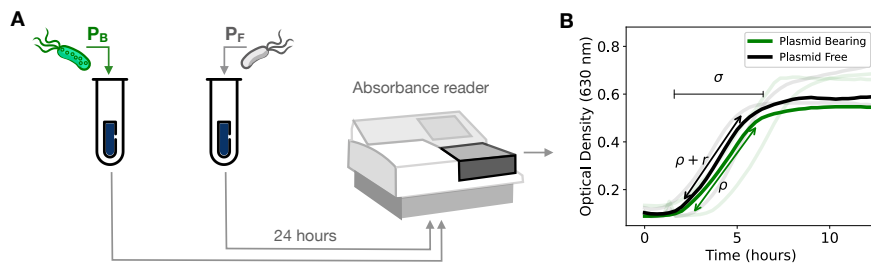
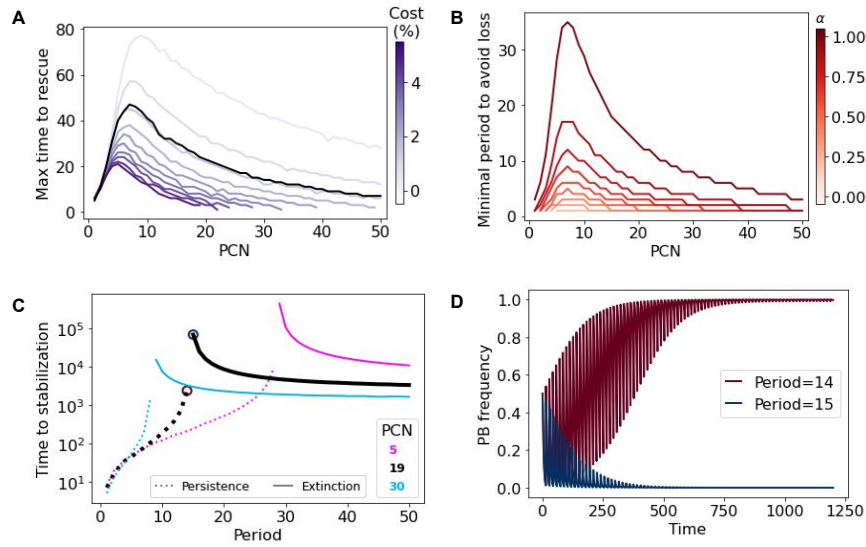
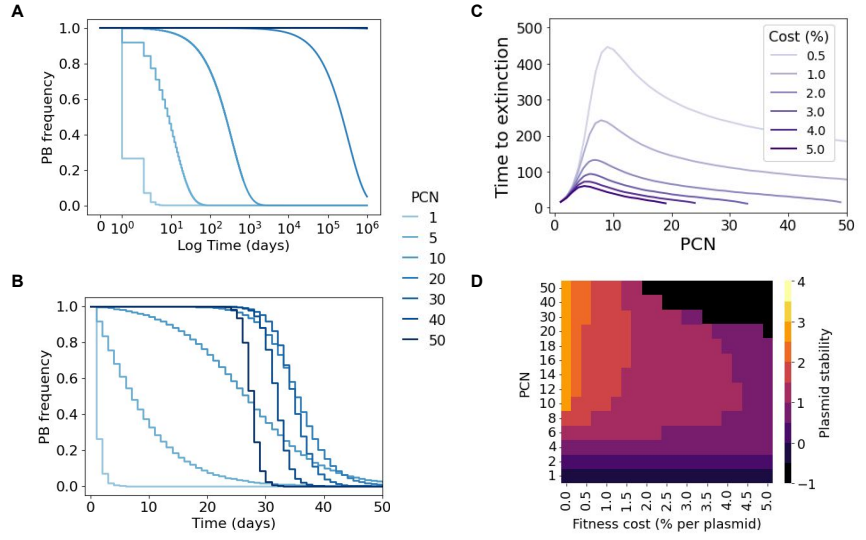
<sup>4</sup>UNAM

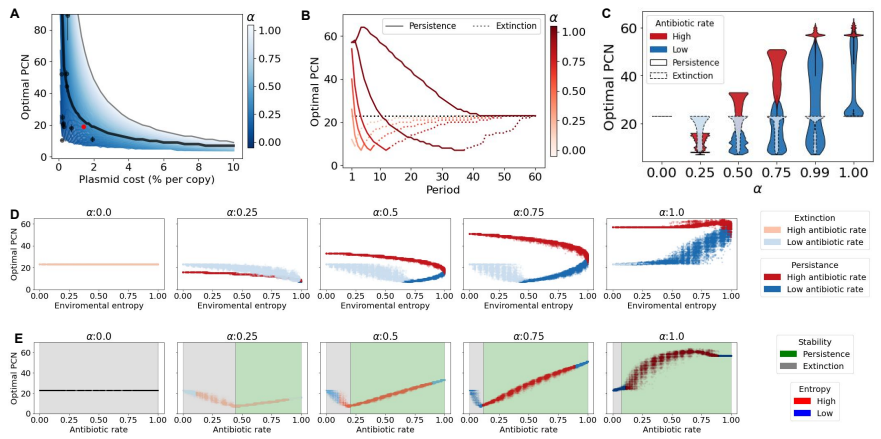
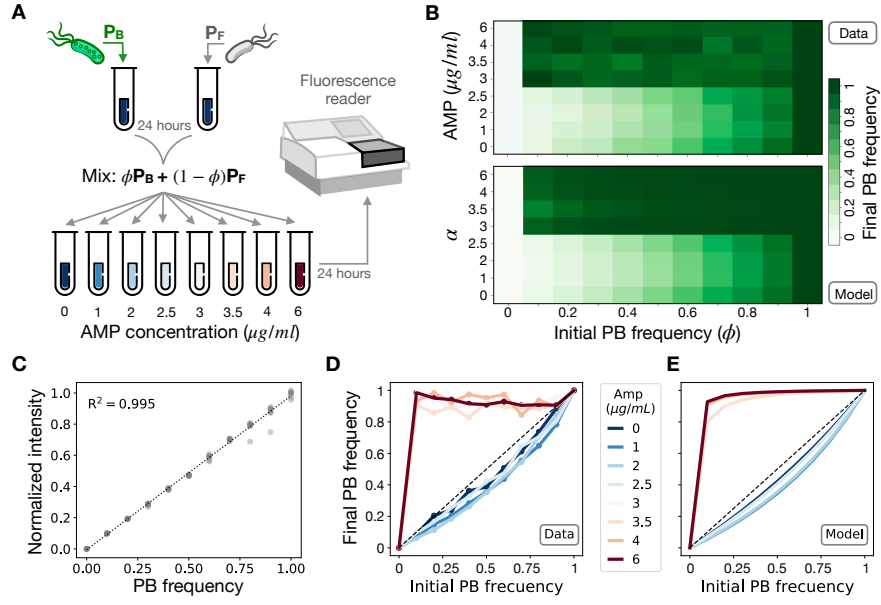
October 8, 2022

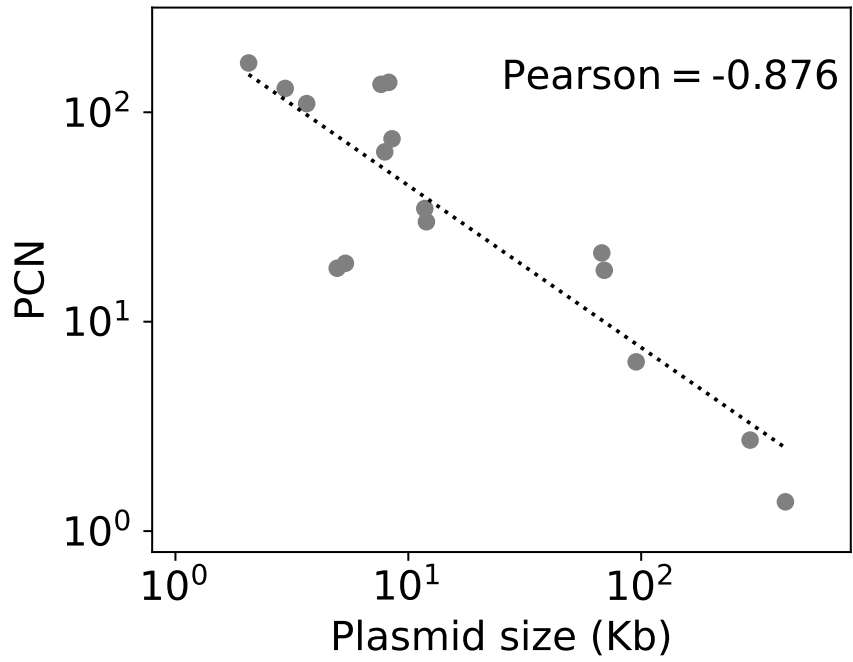
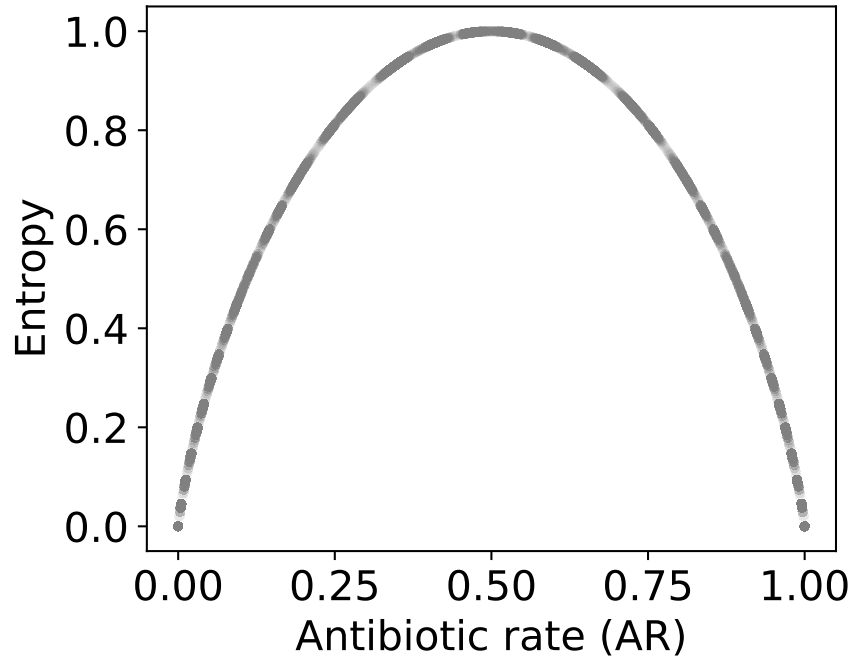
## Abstract

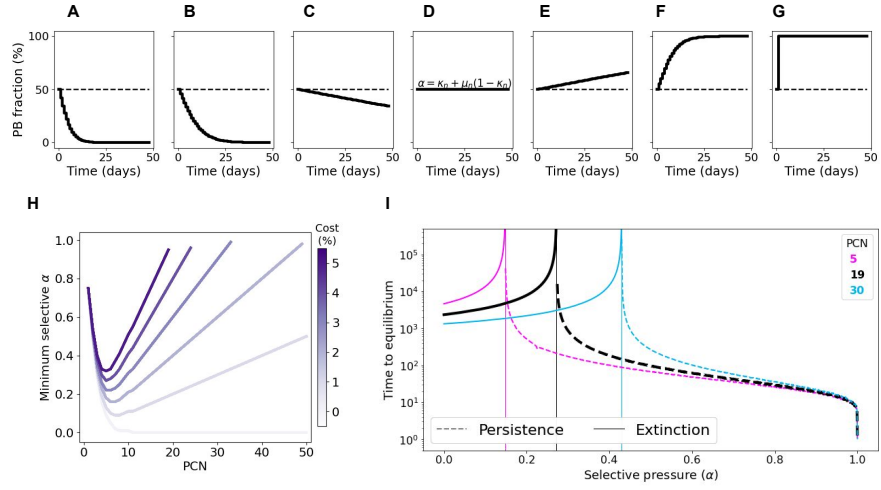
Plasmids are extra-chromosomal genetic elements that encode a wide variety of phenotypes and can be maintained in bacterial populations through vertical and horizontal transmission, thus increasing bacterial adaptation to hostile environmental conditions like those imposed by antimicrobial substances. To circumvent the segregational instability resulting from randomly distributing plasmids between daughter cells upon division, non-transmissible plasmids tend to be carried in multiple copies per cell, which also results in a metabolic burden to the bacterial host, therefore reducing the overall fitness. This trade-off poses an existential question for plasmids: What is the optimal plasmid copy number? We address this question using a combination of population genetics modeling with microbiology experiments consisting of *Escherichia coli* K12 bearing a multi-copy plasmid encoding for blaTEM-1, a gene conferring resistance to b-lactam antibiotics. We use a Wright-Fisher model to evaluate the interaction between the above mentioned opposing forces. By numerically determining the optimal plasmid copy number for constant and fluctuating selection regimes, we conclude that plasmid copy number is an optimized evolutionary trait that depends on the rate of environmental fluctuation and balances the benefit between increased stability in the absence of selection with the burden associated with carrying multiple copies of the plasmid.











# Segregational instability of multicopy plasmids: a population genetics approach

JCR Hernández<sup>1,2,†</sup>, V Miró Pina<sup>3,4,5,†</sup>, A Siri-Jégousse<sup>5</sup>, R Peña-Miller<sup>1</sup>, S Palau<sup>5</sup>, and A González Casanova<sup>6</sup>

<sup>1</sup> Laboratorio de Biología de Sistemas, Centro de Ciencias Genómicas, Universidad Nacional Autónoma de México, 62210, Cuernavaca, México.

<sup>2</sup> Department of Microbial Population Biology, Max Planck Institute for Evolutionary Biology, 24306 Plön, Germany.

<sup>3</sup> Centre for Genomic Regulation (CRG), The Barcelona Institute of Science and Technology, Barcelona, Spain.

<sup>4</sup> Universitat Pompeu Fabra (UPF), Barcelona, Spain.

<sup>5</sup> Departamento de Probabilidad y Estadística, Instituto de Investigación en Matemáticas Aplicadas y en Sistemas, Universidad Nacional Autónoma de México, México.

<sup>6</sup> Instituto de Matemáticas, Universidad Nacional Autónoma de México, México. Corresponding author: adriangcs@matem.unam.mx

<sup>†</sup>These two authors contributed equally to this work and are listed in alphabetical order

## ABSTRACT

1

2

3 Plasmids are extra-chromosomal genetic elements that encode a wide variety of phenotypes and can  
4 be maintained in bacterial populations through vertical and horizontal transmission, thus increasing  
5 bacterial adaptation to hostile environmental conditions like those imposed by antimicrobial sub-  
6 stances. To circumvent the segregational instability resulting from randomly distributing plasmids  
7 between daughter cells upon division, non-transmissible plasmids tend to be carried in multiple  
8 copies per cell, with the added benefit of exhibiting increased gene dosage and resistance levels.  
9 But carrying multiple copies also results in a high metabolic burden to the bacterial host, therefore  
10 reducing the overall fitness of the population. This trade-off poses an existential question for plasmids:  
11 What is the optimal plasmid copy number? In this manuscript, we address this question by postulating  
12 and analyzing a population genetics model to evaluate the interaction between selective pressure,  
13 the number of plasmid copies carried by each cell, and the metabolic burden associated with plasmid  
14 bearing in the absence of selection for plasmid-encoded traits. Parameter values of the model were  
15 estimated experimentally using *Escherichia coli* K12 carrying a multicopy plasmid encoding for a  
16 fluorescent protein and *bla*<sub>TEM-1</sub>, a gene conferring resistance to  $\beta$ -lactam antibiotics. By numerically  
17 determining the optimal plasmid copy number for constant and fluctuating selection regimes, we  
18 show that plasmid copy number is a highly optimized evolutionary trait that depends on the rate of  
19 environmental fluctuation and balances the benefit between increased stability in the absence of  
20 selection with the burden associated with carrying multiple copies of the plasmid.

21 Keywords: Population genetics, Plasmid dynamics, Experimental microbiology

## 22 1 Introduction

23 Prokaryotes transfer DNA at high rates within microbial communities through mobile genetic elements  
24 such as bacteriophages,<sup>1</sup> transposons<sup>2</sup> or extra-chromosomal DNA molecules known as plasmids.<sup>3</sup>  
25 Crucially, plasmids have core genes that allow them to replicate independently of the chromosome but  
26 also encode for accessory genes that provide their bacterial hosts with new functions and increased  
27 fitness in novel or stressful environmental conditions.<sup>4</sup> Plasmids have been widely studied due to their  
28 biotechnological potential<sup>5</sup> and their relevance in agricultural processes,<sup>6</sup> but also because of their  
29 importance in clinical practice since they have been identified as significant factors contributing to the  
30 current global health crisis generated by drug resistant bacterial pathogens.<sup>7</sup>

31 Although the distribution of plasmid fitness effects is variable and context dependant,<sup>8</sup> it is generally  
32 assumed that in the absence of selection for plasmid-encoded genes, plasmids impose a fitness burden  
33 on their bacterial hosts.<sup>9,10</sup> As a result, plasmid-bearing populations can have a competitive disad-  
34 vantage compared to plasmid-free cells, thus threatening plasmids to be cleared from the population  
35 through purifying selection.<sup>11</sup> To avoid extinction, some plasmids can transfer horizontally to lineages  
36 with increased fitness, with previous theoretical results establishing sufficient conditions for plasmid  
37 maintenance, namely that the rate of horizontal transmission has to be larger than the combined effect  
38 of segregational loss and fitness cost.<sup>12,13</sup> Also, some plasmids encode molecular mechanisms that  
39 increase their stability in the population, for instance, toxin-antitoxin systems that kill plasmid-free  
40 cells,<sup>14</sup> or active partitioning mechanisms that ensure the symmetric segregation of plasmids upon  
41 division.<sup>15</sup>

42 To avoid segregational loss, non-conjugative plasmids lacking active partitioning and post-segregational  
43 killing mechanisms tend to be present in many copies per cell, therefore decreasing the probability  
44 of producing a plasmid-free cell when randomly segregating plasmids during cell division. But this  
45 reduced rate of segregational loss is not sufficient to explain the stable persistence of costly plasmids in  
46 the population, suggesting that a necessary condition for plasmids to persist in the population is to carry  
47 beneficial genes for their hosts that are selected for in the current environment. However, regimes that  
48 positively select for plasmid-encoded genes can be sporadic and highly specific, so plasmid persistence  
49 is not guaranteed in the long term. Moreover, even if a plasmid carries useful genes for the host, these  
50 can be captured by the chromosome, thus making plasmids redundant and rendering them susceptible to  
51 be cleared from the population.<sup>16</sup> This evolutionary dilemma has been termed the ‘plasmid paradox’.<sup>17</sup>

In this paper, we use a population genetics modeling approach to evaluate the interaction between the number of plasmid copies contained in each cell and the energetic cost associated with carrying each plasmid copy. We consider a non-transmissible, multicopy plasmid (it can only be transmitted vertically) that lacks active partitioning or post-segregational killing mechanisms (plasmids segregate randomly upon division). We will also consider that plasmids encode a gene that increases the probability

53  
54  
55  
56  
57  
58  
59  
60  
61

of survival to an otherwise lethal concentration of an antimicrobial substance, albeit imposing a burden to plasmid-bearing cells in drug-free environments. To estimate parameters of our population genetics model, we used an experimental model system consisting on *Escherichia coli* bearing a multicopy plasmid pBGT (~19 copies per cell) carrying *bla*<sub>TEM-1</sub>, a drug-resistance gene that produces a  $\beta$ -lactamase that degrades ampicillin and other  $\beta$ -lactam antibiotics.<sup>7,18</sup>

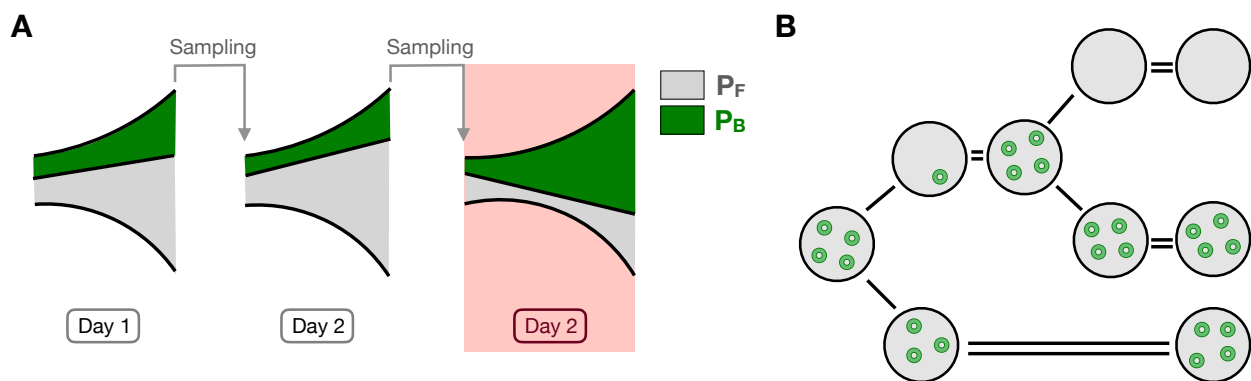
62 We used computer simulations to evaluate the stability of a multicopy plasmid in terms of the  
 63 duration and strength of selection in favor of plasmid-encoded genes. This allowed us to numerically  
 64 estimate the number of copies that maximized plasmid stability under different environmental regimes:  
 65 drug-free environments, constant exposure to a lethal drug concentration, and intermittent periods of  
 66 selection. Altogether, our results confirm the existence of two opposing evolutionary forces acting on  
 67 the number of copies carried by each cell: selection against high-copy plasmids consequence of the  
 68 fitness cost associated with bearing multiple copies of a costly plasmid and purifying selection resulting  
 69 from the increased probability of plasmid loss observed in low-copy plasmids.

## 70 Methods

### 71 1.1 Serial dilution protocol

72 We consider a serial dilution experiment with two types of bacteria: plasmid-bearing (PB) and plasmid-  
 73 free (PF). Let us denote by  $n$  the plasmid copy number (PCN) and argue that this is an important  
 74 parameter: in the one hand, the selective disadvantage of PB individuals due to the cost of carrying  
 75 plasmids is assumed to be proportional to  $n$ ; on the other hand, the PCN determines the heritability of  
 76 the plasmid.

77 In our schema, each day starts with a population of  $N$  cells that grow exponentially until saturation  
 78 is reached (i.e. until there are  $\gamma N$  cells). At the beginning of the next day,  $N$  cells are sampled (at  
 79 random), transferred to new media and exponential growth starts again (Figure 1A).



80  
 81 **Figure 1. Schematic diagram of the model.** **A)** Serial dilution protocol. PB cell are represented in green  
 82 while PF cells are represented in gray. We show three days of the experiments. An antibiotic pulse is added  
 83 during day 3. **B)** Segregational loss. Upon cell division, plasmids are segregated at random between the two  
 84 daughter cells. Then the plasmids are replicated until the PCN is 4. When a cell inherits no plasmid, it becomes  
 86 plasmid free.

## 87 1.2 Inter-day dynamics

88 To model the inter-day dynamics, we consider a discrete-time model in which the population size is  
 89 fixed to  $N$ . Day  $i$  starts with a fraction  $X_i$  of PB cells (and  $1 - X_i$  of PF cells). We consider that the  
 90 fitness cost associated with plasmid maintenance,  $\kappa_n$  is proportional to the PCN, i.e.  $\kappa_n = \kappa n$ . This  
 91 means that, at the end of day  $i$ , the number of PF cells is proportional to their initial frequency  $1 - X_i$ ,  
 92 while the number of PB cells is proportional to their initial frequency  $X_i$  multiplied by  $(1 - \kappa_n) < 1$ . So,  
 93 at the end of day  $i$ , the fraction of PB cells would be

$$94 \frac{(1 - \kappa_n)X_i}{95 (1 - \kappa_n)X_i + 1 - X_i}.$$

97 In addition, PB cells can lose their plasmids and become PF and with probability  $\mu_n$ , so, at the end of  
 98 day  $i$ , the fraction of PB cells needs to be multiplied by  $(1 - \mu_n)$ .

99 At the beginning of day  $i + 1$ , we sample  $N$  individuals at random from the previous generation.  
 100 Since  $N$  is very large, we can neglect stochasticity and assume that the fraction of PB cells at the  
 101 beginning of day  $i + 1$  is equal to their fraction at the end of day  $i$ , i.e.

$$102 X_{i+1} = f(X_i) := \frac{(1 - \kappa_n)X_i}{(1 - \kappa_n)X_i + 1 - X_i} (1 - \mu_n), \quad i \geq 1. \quad (1)$$

105 Additionally, we aim to modeling selection for plasmid-encoded genes. For plasmids carrying  
 106 antibiotic resistance genes, this is achieved by exposing the population to antibiotic pulses. Individuals  
 107 with no plasmids suffer more from this this treatment so, at each pulse, we observe an increment in the  
 108 relative frequency of the PB subpopulation. To model this phenomenon, we assume that, in the presence  
 109 of antibiotic, PF individuals exhibit a selective disadvantage represented by parameter  $\alpha \in [0, 1]$ .

110 For instance, if an antibiotic pulse occurs at day  $i$ , all PB cells survive, (there are  $NX_i$ ), but the PF  
 111 cells die with probability  $\alpha$ , so only  $N(1 - \alpha)(1 - X_i)$  survive. So, the fraction of PB individuals, right  
 112 after the antibiotic pulse becomes

$$113 g(X_i) := \frac{X_i}{114 X_i + (1 - \alpha)(1 - X_i)}.$$

116 Then, cells grow exponentially again, as in a normal day, so that, at the end of the day, the fraction of  
 117 PB cells is  $f(g(X_i))$ .

118 If we consider that the pulses occur at generations  $T, 2T, \dots$ , the frequency process becomes

$$119 X_{i+1} = \begin{cases} 120 f(g(X_i)) = \frac{(1 - \kappa_n)X_i}{1 - \alpha + (\alpha - \kappa_n)X_i} (1 - \mu_n) & \text{if } i = jT, \quad j = 1, 2, \dots \\ 121 f(X_i) = \frac{(1 - \kappa_n)X_i}{(1 - \kappa_n)X_i + 1 - X_i} (1 - \mu_n) & \text{otherwise.} \end{cases} \quad (2)$$

### 1.3 Intra-day dynamics

For the intra-day dynamics, day  $i$  starts with a population of  $N$  cells ( $N \sim 10^5$  in the experiment) that grow exponentially until saturation is reached (i.e. until there are  $\gamma N$  cells.). The initial fraction of PB cells is  $X_i$ . We assume that, in the absence of antibiotic, the population evolves as a continuous time multi-type branching process  $\mathbf{Z}_t = (Z_t^0, Z_t^1)$ , where  $Z_t^0$  (resp  $Z_t^1$ ) is the number of PB cells (resp. PF cells). The reproduction rate (or *Malthusian fitness*) of PB (resp. PF) individuals is  $r$  (resp.  $r + \rho_n$ ), with  $\rho_n > 0$  (since PB individuals have some disadvantage due to the cost of plasmid maintenance). Following<sup>19</sup>, we assume that  $\rho_n \sim N^{-b}$  for some  $b \in (0, 1/2)$  (this regime is known as *moderate-strong selection*).

We consider plasmids that lack active partitioning systems<sup>20</sup> so, at the moment of cell division, each plasmid randomly segregates into one of the two new cells. Once in the new host, the plasmids replicates until reaching  $n$  copies. If, however, one of the two new cells has all the  $n$  copies, the other one will not carry any plasmid copy and becomes PF. Thus, we make the simplifying assumption that the daughter of a PB cell becomes PF with probability  $2^{-n}$  (segregational loss rate), as illustrated in [Figure 1B](#). Therefore, at every branching event, an individual splits in two. Plasmid-free individuals only split in two PF individuals. Plasmid-bearing individuals can split in one PF individual and one PB individual with probability  $2^{-n}$  (if all the plasmids go to one of them) or they can split in two plasmid-bearing individuals with probability  $1 - 2^{-n}$ .

Let  $M(t) = \{M_{i,j}(t) : i, j = 0, 1\}$  be the mean matrix given by  $M_{i,j}(t) = \mathbb{E}_{\mathbf{e}_i}(Z_t^j)$ , the average size of the type  $j$  population at time  $t$  if we start with a type  $i$  individual. According to [21, Section V.7.2],  $M(t)$  can be calculated as an exponential matrix

$$M(t) = e^{tA} \quad \text{where} \quad A = \begin{pmatrix} r + \rho_n & 0 \\ r2^{-n} & r(1 - 2^{-n}) \end{pmatrix}.$$

More precisely,

$$M(t) = \begin{pmatrix} e^{(r+\rho_n)t} & 0 \\ \frac{r2^{-n}}{r2^{-n}+\rho_n}(e^{(r+\rho_n)t} - e^{r(1-2^{-n})t}) & e^{r(1-2^{-n})t} \end{pmatrix}.$$

Let  $\sigma$  be the duration of the growth phase. Since  $N$  is very large, one can assume that reproduction is stopped when the expectation of the number of descendants reaches  $\gamma N$ , i.e. that  $\sigma$  satisfies

$$\begin{aligned} \gamma N &= (1 - X_i)N(M_{0,0}(\sigma) + M_{0,1}(\sigma)) + xN(M_{1,0}(\sigma) + M_{1,1}(\sigma)) \\ &= Ne^{r\sigma} \left( e^{\rho_n\sigma} + \rho_n X_i \frac{e^{-r2^{-n}\sigma} - e^{\rho_n\sigma}}{r2^{-n} + \rho_n} \right). \end{aligned}$$

152

153

154

155 Since  $\rho_n \sim N^{-b}$ , we have for large enough  $N$  that

156

157

$$\sigma \simeq \frac{\log \gamma}{r}.$$

158

Since  $\gamma N \gg 1$ , we can assume that the number of PB (resp. PF) cells at the end of the day is equal to its expected value. Therefore, the fraction of PB cells at the end of day  $i$  is equal to

159

160

161

$$\frac{X_i M_{1,1}(\sigma)}{(1 - X_i)(M_{0,0}(\sigma) + M_{0,1}(\sigma)) + X_i(M_{1,0}(\sigma) + M_{1,1}(\sigma))} = \frac{X_i e^{-(r2^{-n} + \rho_n)\sigma}}{(1 - X_i) + X_i \frac{r2^{-n} + \rho_n e^{-(r2^{-n} + \rho_n)\sigma}}{r2^{-n} + \rho_n}}. \quad (3)$$

162

This corresponds to equation (2) with parameters

163

164

165

166

$$\kappa_n = \frac{\rho_n(1 - e^{-(r2^{-n} + \rho_n)\sigma})}{r2^{-n} + \rho_n} \sim \sigma \rho_n = \sigma \rho_n \quad \text{and} \quad \mu_n = 1 - \frac{r2^{-n} + \rho_n}{r2^{-n} e^{(r2^{-n} + \rho_n)\sigma} + \rho_n} \sim_{n \rightarrow \infty} r \sigma 2^{-n}. \quad (4)$$

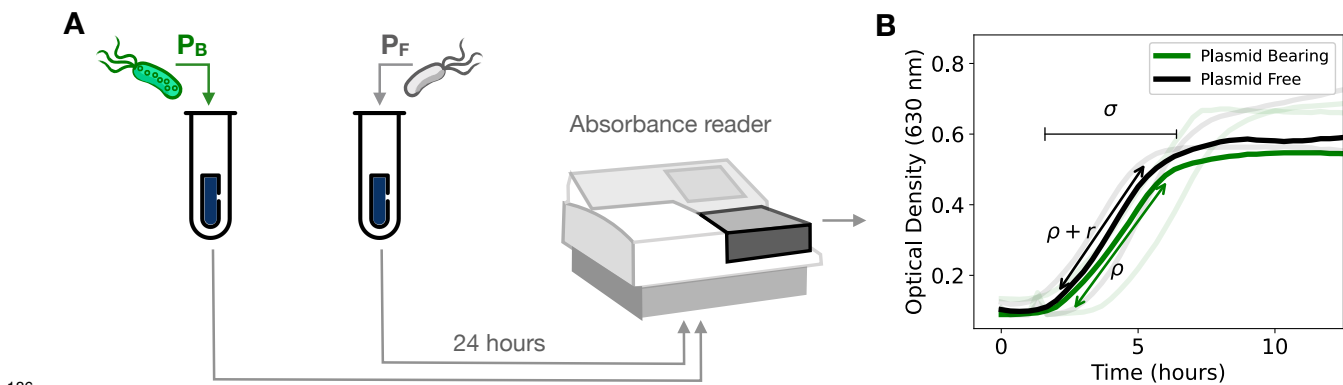
167

168 The importance of these formulas is that they connect measurable quantities with theoretical parameters,  
 169 leading to a method to estimate the parameters of the model from experiments, which is the spirit of  
 170 the experiment described in the following section.

## 171 1.4 Model parametrization

172 Our goal is to use the inter-day model to evaluate the long-term dynamics of plasmid-bearing populations  
173 in terms of the cost associated with carrying plasmids and the fitness advantage conferred by the plasmid  
174 in the presence of positive selection. To quantify these parameters experimentally, our approach  
175 consisted in two phases: (1) from growth kinetic experiments, we estimate parameters  $\rho$ ,  $r$  and  $\sigma$  of  
176 the inter-day model, and (2) we perform competition experiments in a range of drug concentrations to  
177 obtain  $\mu_n$  and  $\kappa_n$  using equation (4) of the intra-day model.

178 Our experimental model system consisted in *Escherichia coli* K12 carrying pBGT, a non-transmissible  
179 multicopy plasmid used previously to study plasmid dynamics and drug resistance evolution.<sup>22–25</sup>  
180 Briefly, pBGT is a ColE1-like plasmid with  $\sim 19$  plasmid copies per cell, lacking the necessary machin-  
181 ery to perform conjugation or to ensure symmetric segregation of plasmids upon division. This plasmid  
182 carries a GFP reporter under an arabinose-inducible promoter and the *bla*<sub>TEM-1</sub> gene that encodes  
183 for a  $\beta$ -lactamase that efficiently degrades  $\beta$ -lactam antibiotics, particularly ampicillin (AMP). The  
184 minimum inhibitory concentration (MIC) of PB cells to AMP is 8,192 mg/l, while the PF strain has a  
185 MIC of 4 mg/l (see [Appendix A](#)).



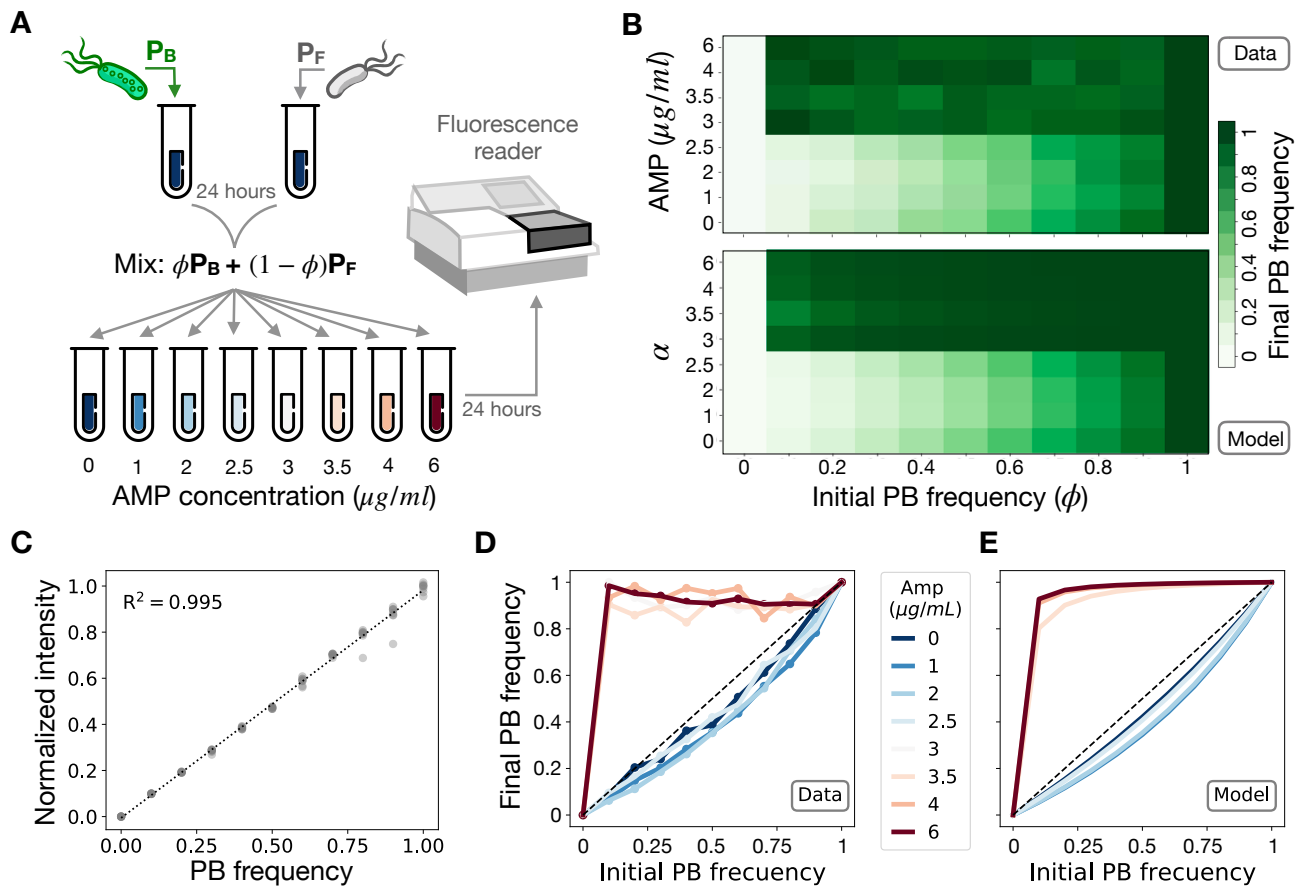
187 **Figure 2. Growth kinetic experiment.** A) Schematic diagram illustrating a bacterial growth experiment  
188 performed in drug-free media separately for PB and PF populations. We used an absorbance microplate reader to  
189 measure the optical density (OD<sub>630</sub>) at different time-points during the 24-hour experiment. B) Growth curves of  
190 PB (green) and PF (black) strains, with replicate experiments represented as shaded curves. The duration of the  
191 exponential phase,  $\sigma$ , was estimated by identifying the start of exponential phase and the time elapsed before  
192 reaching carrying capacity. Parameter  $\rho$  refers to the maximum growth rate of the PB population, while the  
193 selective advantage of the PF strain is represented with  $r$ .

195 Growth experiments were performed in 96-well plates with lysogeny broth (LB) rich media and  
196 under controlled environmental conditions. Using an plate absorbance spectrophotometer, we obtained  
197 bacterial growth curves that enabled us to estimate the maximal growth rate of the PB and PF strains,  
198 corresponding to  $r$  and  $\rho_n$  in the intra-day model<sup>26</sup> (Figure 2A and Appendix C). As expected, we  
199 observed a reduction in bacterial fitness of the PB subpopulation, expressed in terms of a decrease in its  
200 maximum growth rate when grown in isolation. The metabolic burden associated with carrying the  
201 pBGT plasmid ( $n = 19$ ) was estimated at  $0.108 \pm 0.067$  (Figure 2B).

202 We then performed a one-day competition experiment consisting of mixing PB and PF subpopula-  
203 tions with a range of relative abundances and exposing the mixed populations to environments with  
204 increasing drug concentrations (see Figure 3A for a schematic of the experimental protocol). Previous  
205 studies have used a similar approach to determine a selection coefficient,<sup>27</sup> a quantity that was used  
206 to show that selection of resistance can occur even at sub-lethal antibiotic concentrations.<sup>28</sup> Figure  
207 3B shows the final PF frequency obtained for different initial population structures and strengths of  
208 selection.

209 The fitness cost associated with carrying plasmids in our inter-day model was estimated from the  
210 proportion of PB cells at the end of a competition experiment. This quantity can be obtained from the  
211 normalized fluorescent intensity of the bacterial culture, measured with a fluorescent spectrophotometer  
212 or with flow cytometry (Figure 3C shows a linear relationship between both quantities). Figure 3D  
213 shows the end-point bacterial density resulting from competition experiments with different initial  
214 fractions of PB cells exposed to a range of AMP concentrations. Note that, at low AMP concentrations  
215 (blue lines), the frequency of plasmid-bearing is below the identity, consistent with plasmids imposing  
216 a fitness cost to PB cells. In contrast, at high AMP concentrations (red lines), plasmid-free cells are  
217 killed and the population is almost exclusively conformed by PB cells.

218 In the model, since PCN is a fixed parameter, the PB fraction resulting from a competition  
219 experiment in the absence of selection only depends on the cost associated with plasmid bearing.  
220 Therefore, by fitting equation (1), we estimated that the cost associated with carrying  $n = 19$  copies  
221 of pBGT was  $\kappa_n = 0.272$ . Furthermore, by fixing this parameter and incorporating antibiotics, we  
222 estimated the selective pressure  $\alpha$  for different antibiotic concentrations by fitting equation (2) to  
223 the experimental data. Figure 3E illustrates that at low antibiotic concentrations (small values of  $\alpha$ )  
224 the frequency of the population is low, while higher values of  $\alpha$  result in an increased PB frequency.  
225 Table 1 summarizes parameter values estimated for each strain in our model, and Table 2 shows the  
226 correspondence between antibiotic concentrations and  $\alpha$ .



227

228 **Figure 3. Competition experiment under a range of drug concentrations.** **A)** Schematic diagram  
 229 illustrating an experiment where PB and PF are mixed at different relative abundances and submitted to a range  
 230 of ampicillin concentrations (0, 1, 2, 2.5, 3, 3.5, 4, and 6  $\mu\text{g/ml}$ ). We use a fluorescence spectrophotometer to  
 231 estimate the relative abundance of plasmid bearing cells in the population after 24 hours of growth. **B)** Final PF  
 232 frequency (illustrated in a gradient of green) for different initial fraction of PB cells and selection coefficients  
 233 (top: data; bottom: model). **C)** Control experiment illustrating that normalized fluorescence intensity is  
 234 correlated with the fraction of the population carrying plasmids. Each dot present a replica and the dotted line a  
 235 linear regression ( $R^2=0.995$ ). **D)** Experimental iterative map showing the existence of a minimum drug  
 236 concentration that rescues the PB population (red lines). At low drug concentrations (blue lines), the PB  
 237 population decreases in frequency. **E)** Theoretical iterative map obtained by numerically solving equation (2)  
 238 for a range of strength of selections and initial PB frequencies. By fixing  $\kappa_n$  (previously estimated by growing each  
 239 strain in monoculture), we fitted parameter  $\alpha$  in equation (2) to the experimental data. Colors indicate the  
 240 strength of selection (in blue, values of  $\alpha$  where the cost of carrying plasmids is stronger than the benefit  
 241 resulting from positive selection, yielding curves below the identity line. Red curves represent simulations  
 242 obtained with values of  $\alpha$  strong enough to kill PF cells, thus increasing PB frequency in the population.

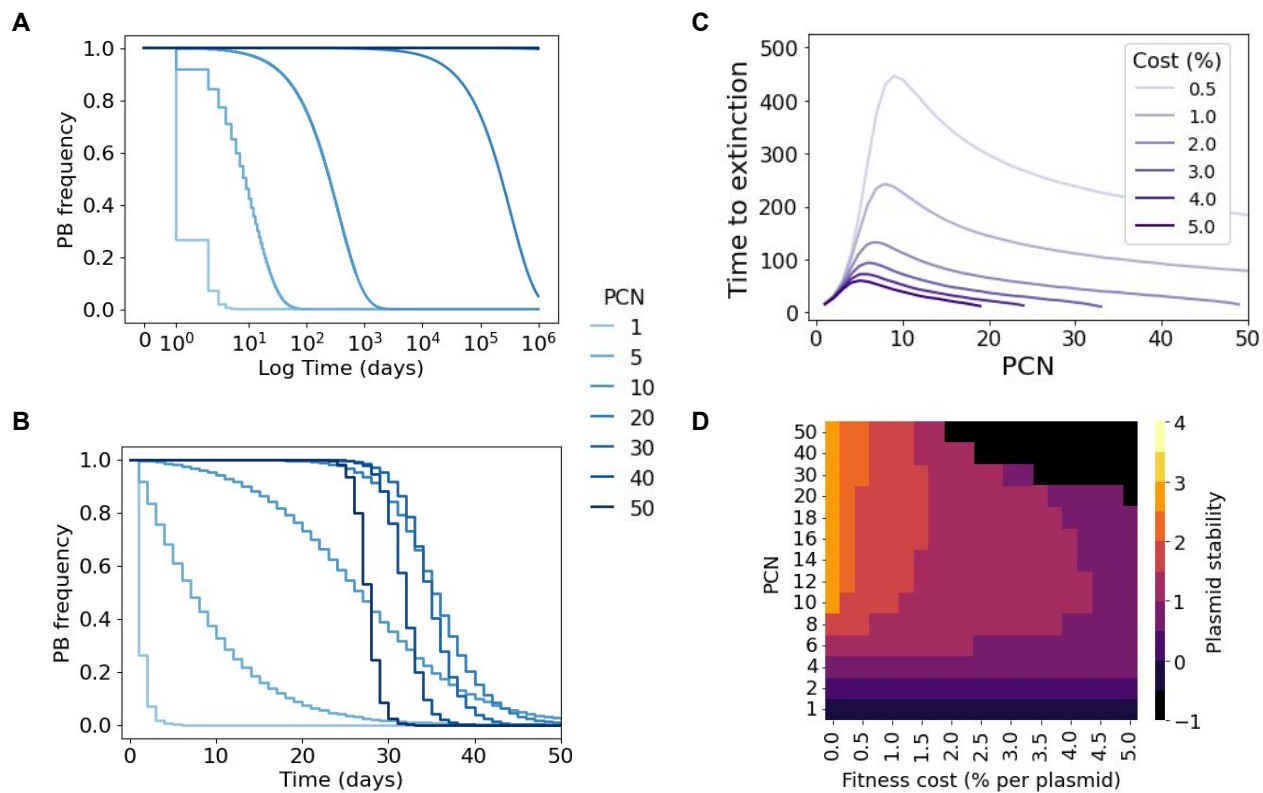
## 244 **2 Results**

### 245 **2.1 Segregational instability in the absence of selection**

246 Our first aim was to evaluate the stability of a costly multicopy plasmid in the absence of selection for  
247 plasmid-encoded genes (i.e. without antibiotics). By numerically solving equation (1), we evaluated the  
248 stability of the PB subpopulation in terms of the mean PCN and the fitness cost associated with carrying  
249 each plasmid copy (see [Appendix C](#)). As expected, in the absence of selection, plasmids are always  
250 cleared from the population with a decay rate that depends on PCN. We define the time-to-extinction as  
251 the time when the fraction of PB cells goes below an arbitrary threshold.

253 For cost-free plasmids (i.e. when  $\kappa = 0$ ), the time-to-extinction appears to be correlated to PCN  
254 ([Figure 4A](#)). In contrast, if we consider a costly plasmid ( $\kappa > 0$ ) and that the total fitness cost is  
255 proportional to the PCN (i.e. if  $PCN = n$ , the total cost is  $\kappa_n = \kappa n$ ), then extinction occurs in a much  
256 faster timescale ([Figure 4B](#) – notice the difference of timescales with [Figure 4A](#)). As shown in [Figure](#)  
257 [4B](#), small PCN values are associated with a high probability of segregational loss, and therefore the  
258 time-to-extinction increases with PCN. However, large values of PCN are associated with higher levels  
259 of instability due to the detrimental effect on host fitness resulting from carrying multiple copies of a  
260 costly plasmid.

261 This observation indicates the existence of a non-linear relationship between stability of plasmids  
262 and the mean PCN of the population. To further explore this association, we computationally estimated  
263 the time-to-extinction in a long-term setting (simulations running up to 500 days) for different values  
264 of PCN and fitness cost. As expected, [Figure 4C](#) shows an accelerated rate of plasmid loss in costly  
265 plasmids. Crucially, there appears to be a critical PCN that maximizes the time-to-extinction, that  
266 depends on the per-cell plasmid cost. The time-to-extinction gives a notion of the stability of plasmids,  
267 but this measure may not apply if we introduce antibiotics, and therefore avoid plasmid extinction.  
268 For this reason, we also quantified plasmid stability by measuring the area under the curve (AUC) of  
269 simulation trajectories similar to those in [Figure 4B](#). The heatmap illustrated in [Figure 4D](#) shows this  
270 measure highlighting the existence of a region in the cost-PCN plane, at intermediary PCN values,  
271 where plasmid stability is maximized.



252

**Figure 4. Numerical results for the model without selection for plasmid-encoded genes.** **A)** Plasmid frequency as a function of time for a cost-free plasmid ( $\kappa = 0$ ). Note how, as the PCN increases, the stability of plasmids also increases, although eventually all plasmids will be cleared from the system. **B)** Dynamics of plasmid loss for strains bearing a costly plasmid ( $\kappa = 0.0143$ ). In this case, low-copy plasmids (light blue lines) are highly unstable, but so are high-copy plasmids (dark blue lines). **C)** Time elapsed before plasmid extinction for a range of PCNs. A very costly plasmid ( $\kappa = 5\%$ ) is represented in dark purple, while the light purple line denotes a less costly plasmid ( $\kappa = 0.5\%$ ). **D)** Plasmid stability for a range of fitness costs and PCNs (discrete colormap indicates level of stability, yellow denotes higher stability, while dark purple denotes rapid extinction). Stability is measured as the area under the curve (AUC) of trajectories similar to those in **B**, expressed in  $\log_{10}$  scale. Notice that, for intermediate fitness costs, the PCN that maximizes plasmid stability can be found at intermediate values.

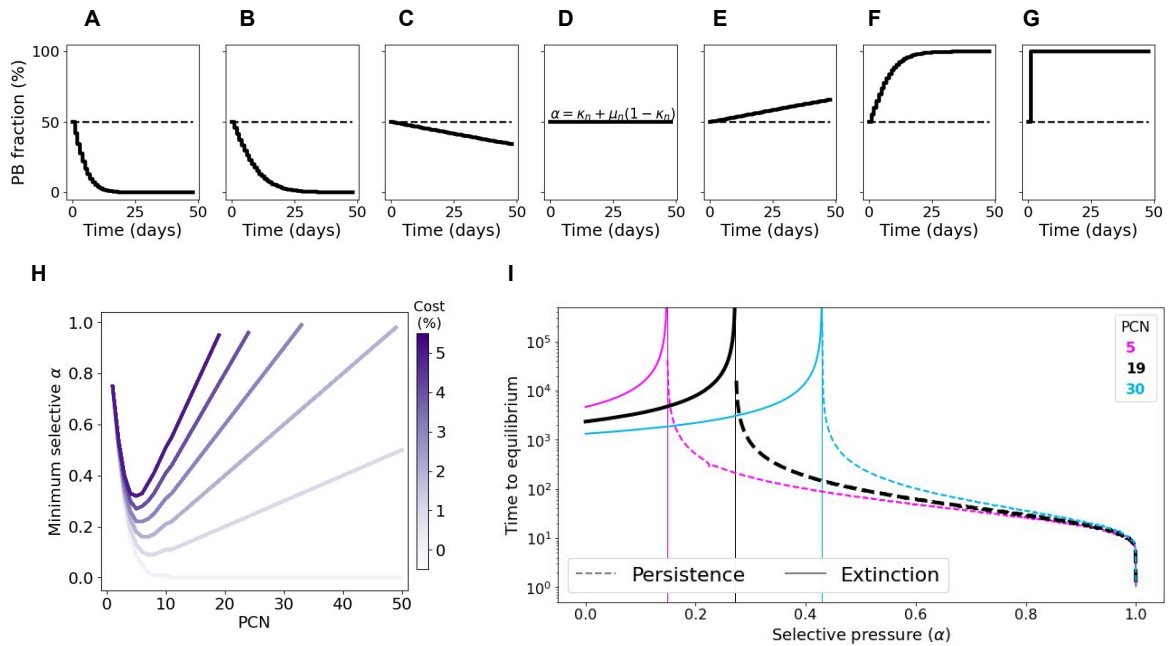
## 272 2.2 Evaluating the role of selection in the stability of plasmids

273 To study the interaction between plasmid stability and the strength of selection in favor of PB cells,  
274 we assumed that the plasmid carries a gene that confers a selective advantage to the host in specific  
275 environments (e.g. resistance to heavy metals or antibiotics). For the purpose of this study, we will  
276 consider a bactericidal antibiotic (e.g. ampicillin) that kills PF cells with a probability that depends  
277 on the antibiotic dose. This results in a competitive advantage of the PB cells with respect to the PF  
278 subpopulation in this environment. We denote the intensity of this selective pressure by  $\alpha$ .

279 [Figures 5A-G](#) illustrate plasmid dynamics over time for different values of  $\alpha$ , obtained numerically  
280 by solving equation (2) with a fixed PCN ( $n = 19$ ) and drug always present in the environment  
281 ( $T = 1$ ). In our model, we found a critical dose that stabilizes plasmids in the population, that is,  
282 the minimum selective  $\alpha$ ,  $MS\alpha = \kappa_n + \mu_n(1 - \kappa_n)$  (see [Appendix B](#)). The existence of a minimum  
283 selective concentration (MSC) that maintains plasmids in the population is a feature used routinely  
284 by bioengineers to stabilize plasmid vectors through selective media.<sup>29</sup> Recall that in our model  
285 the PF MIC is  $\alpha = 1$ , therefore the  $MS\alpha$  can be directly compared to the MSC/MIC ratio previously  
286 proposed<sup>28,30</sup> as a concern factor on selection of resistant strains in the environment.

287 As illustrated in [Figure 5H](#), both low-copy and high-copy plasmids are inherently unstable and  
288 therefore the selective pressure necessary to stabilize them is relatively high, particularly for costly  
289 plasmids. Interestingly, at intermediate PCN values, the selective conditions necessary to stabilize  
290 plasmids are considerably less stringent than for low- and high-copy plasmids. This is the result of  
291 the non-linear relationship between  $MS\alpha$  and  $n$ ; since  $\mu_n$  decreases exponentially with  $n$ , while  $\kappa_n$   
292 increases only linearly with  $n$ .

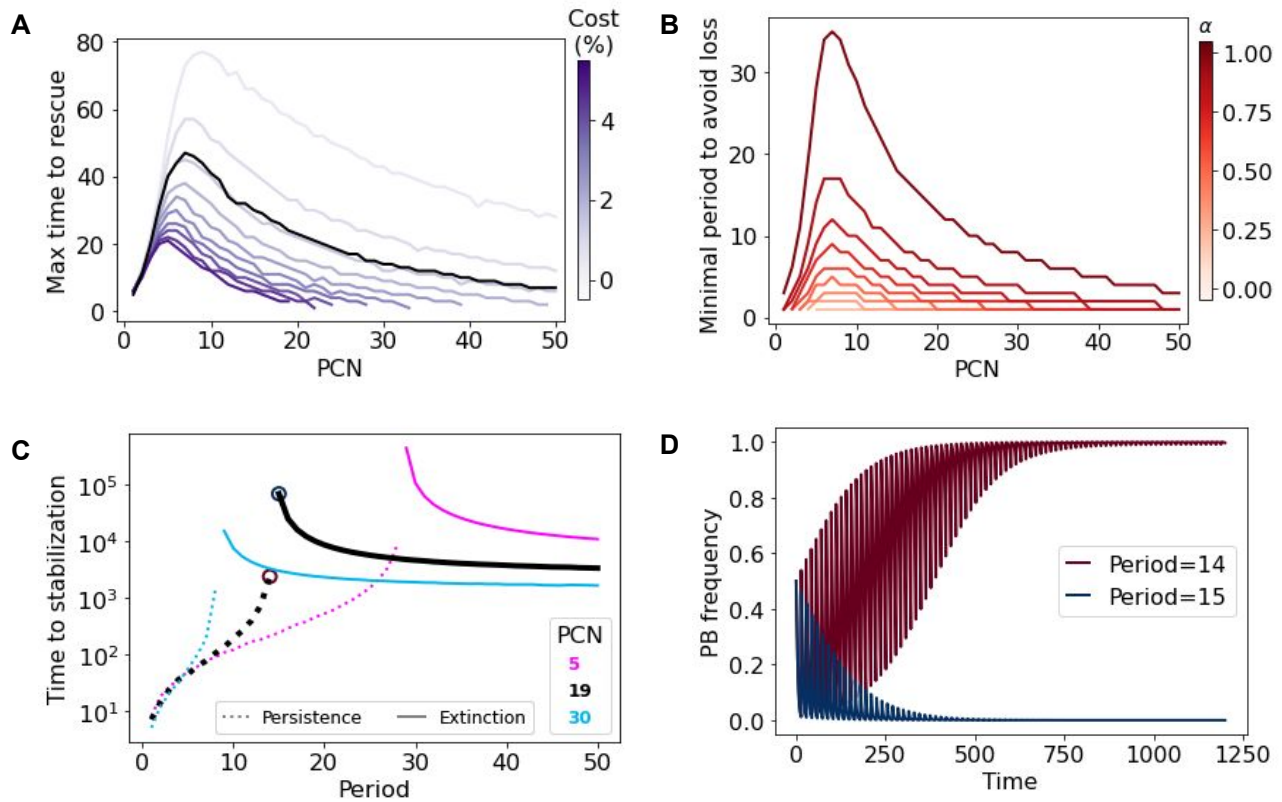
293 [Figure 5I](#) shows the time elapsed before converging to a steady-state (either extinction or persistence)  
294 for different values of  $\alpha$  and PCN. As  $\alpha$  increases, the cost of plasmid-bearing is compensated by the  
295 benefit of carrying the plasmid and therefore plasmids are maintained in the population for longer. Note  
296 that at large values of  $\alpha$ , plasmid-free cells are killed immediately independently of the mean PCN of  
297 the population, resulting very fast in a population composed almost exclusively of plasmid-bearing  
298 cells. Note that, in the case, the steady state  $x^* = 1 - \mu_n \frac{1 - \kappa_n}{\alpha - \kappa_n}$  is achieved independently of the initial  
299 fraction of PB cells (see [Appendix B](#)), which is consistent with previous results.<sup>31</sup>



300  
 301 **Figure 5. Numerical results illustrating the effect of a constant selective pressure in the stability of**  
 302 **non-transmissible multicopy plasmids. A-G)** Each box illustrates the temporal dynamics of the  
 303 plasmid-bearing subpopulation in a pairwise competition experiment inoculated with equal initial fractions of  
 304 *PF* and *PB*. From left to right,  $\alpha = 0, 0.2, 0.26, 0.28, 0.6$  and  $1$ . The dotted line denotes  $MS\alpha = \kappa_n + \mu_n(1 - \kappa_n)$   
 305 for  $n = 19$  and  $\kappa_n = 0.27$ . Note that for values of  $\alpha < MS\alpha$ , plasmids are unstable and eventually cleared from  
 306 the population, while for  $\alpha > MS\alpha$  the plasmid-bearing subpopulation increases in frequency until reaching  
 307 fixation. For  $\alpha = MS\alpha$ , the selective pressure in favor of the plasmid compensates its fitness cost and therefore  
 308 the plasmid fraction remains constant throughout the experiment. **H)** Minimum selective pressure required to  
 309 avoid plasmid loss for a range of PCNs. Different curves represent plasmids with different fitness costs (light  
 310 purple denotes cost-free plasmids and dark purple a very costly plasmid). Note that, for costly plasmids, there  
 311 exists a non-monotone relationship between  $MS\alpha$  and PCN. **I)** Time elapsed before plasmid fraction in the  
 312 population is stabilized, for different copy numbers (5 in magenta, 19 in black, and 30 in cyan). Dotted lines  
 313 represent plasmid fixation, while dashed lines denote stable co-existence between plasmid-free and  
 314 plasmid-bearing subpopulations, and solid lines plasmid extinction. The vertical line indicates  $MS\alpha$ , the  
 315 minimum selective pressure that stably maintains plasmids in the population. Black letters indicate the parameter  
 316 values used in the examples shown in **A-G**.

318 **2.3 Plasmid stability in periodic environments**

319 The purpose of this section is to understand the ecological dynamics of the plasmid-bearing population  
 320 in fluctuating environments, i.e. when periodic antibiotic pulses are administered. We started by  
 321 exploring the time duration a PB population can survive without antibiotics before being rescued by a  
 322 strong antibiotic pulse (Figure 6A). Consistently with the results from the first section, lower plasmid  
 323 costs result in increased rescue times, suggesting that a lesser rate of antibiotic exposure is required for  
 324 their maintenance. In Figure 6B, we quantified this minimal period as a function of PCN and  $\alpha$ . Note  
 325 that higher values of  $\alpha$  correspond to longer periods, which follows from the fact that a higher selective  
 326 pressure increases the PB frequency. Figure 6D illustrates this critical period for  $PCN = 19$ .



327  
 328 **Figure 6. Numerical results of the model in periodic environments.** A) Maximum time a plasmid  
 329 population can grow without antibiotics to avoid plasmid loss when applying a strong antibiotic pulse. Curves  
 330 represent how this time is affected by PCN. Blue intensity represents plasmid cost, and black line indicates  
 331 results using the pBGT parameters. B) Minimal period required to avoid plasmid extinction. Simulations were  
 332 performed using the pBGT measured cost ( $\kappa = 0.014$ ). Red intensity represents different values of  $\alpha$ . Note that  
 333 higher values of  $\alpha$  increase the minimal period. C) Time required for trajectories to stabilize for copy numbers 5,  
 334 19, and 30 using  $\alpha = 0.99$  and the measured cost per plasmid. Note that there is a critical period that defines  
 335 fixation or coexistence marked by red and blue circles on the PCN=19 (black) curve. D) Trajectories for the  
 336 critical periods of PCN=19 starting from 0.5 PB-PF frequency. Note that one day period difference leads to  
 338 opposite outcomes.

339 In periodic environments, the relative abundance of the PB population is driven to zero (extinction)  
340 or reaches a steady state in which the plasmid fraction oscillates around an equilibrium frequency  
341 (persistence). In [Figure 6C](#), times to stabilization were estimated for the strong selection regime  
342 ( $\alpha = 0.99$ ), using the same PCNs as in [Figure 5I](#). Notice that the time-to-extinction is larger than the  
343 time to reach the periodic attractor. In both cases, the maximal time to rescue and the minimum period  
344 to avoid loss, we observe a non-monotone effect of PCN and, therefore, a range of PCNs whereby  
345 plasmid stability is maximized. This is consistent with what we observed without antibiotics ([Figure](#)  
346 [4C](#)) and with constant environments ([Figure 5H](#)).

## 347 **2.4 Optimal PCN depends on the rate of environmental fluctuation**

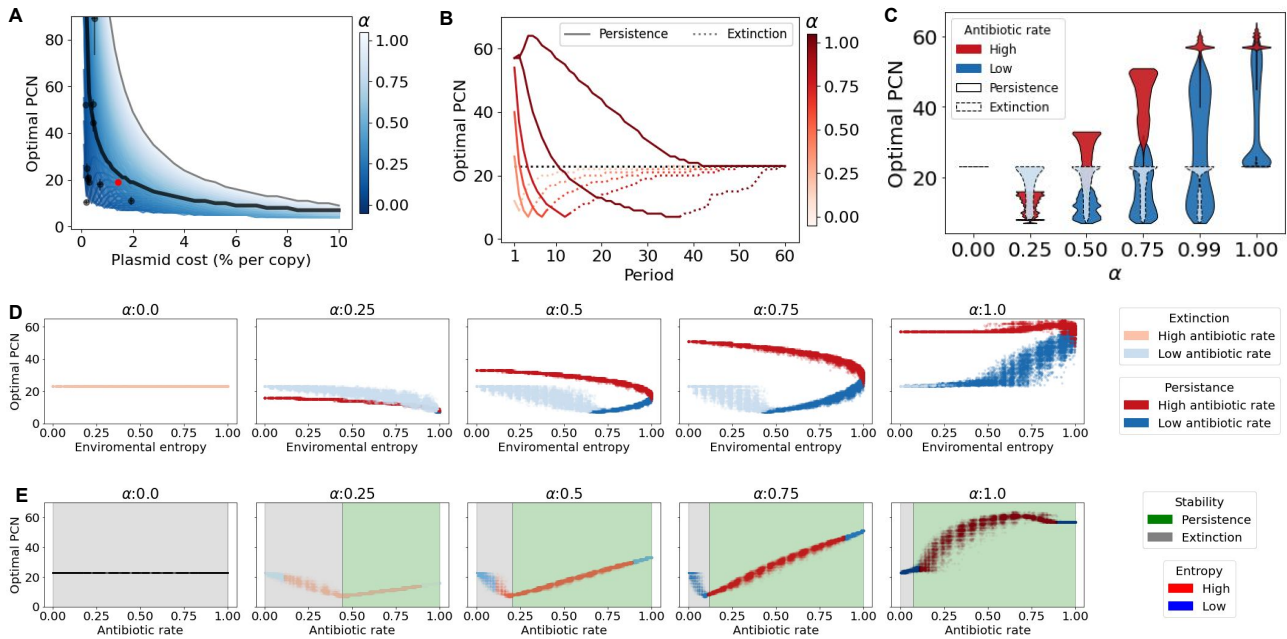
348 In this section, we aim at exploring the concept of optimal PCN and how it depends on the environment.  
349 To do so, we define the optimal PCN (hereafter denoted PCN<sup>\*</sup>) as the PCN that maximizes the area  
350 under the curve (AUC) of the PB frequency over time. This notion of stability was already introduced  
351 in [Figure 4D](#) and has the advantage that it can be used when the PB fraction goes to 0, to a fixed  
352 equilibrium, or when it oscillates.

353 First, we calculated PCN<sup>\*</sup> for a range of plasmids fitness costs in the absence of selection (black  
354 solid line of [Figure 7A](#)) and found that PCN<sup>\*</sup> is inversely correlated with the plasmid fitness cost. In  
355 order to compare the optimal PCN predicted by the model with PCN values found in other experimental  
356 plasmid-host associations, we searched the literature for studies that measure both PCN and fitness cost.  
357 These values are summarized in [Table 3](#) and illustrated in [Figure 7A](#). The values of PCN found in the  
358 literature were below the predicted PCN<sup>\*</sup> in an antibiotic-free regime (black solid line), suggesting that  
359 plasmids would be unstable in the absence of selection. But, crucially, PCN values obtained from the  
360 literature are within the blue-shaded area that represents the PCN<sup>\*</sup> estimated for different environments  
361 (observe the non-linear relationship between  $\alpha$ , PCN<sup>\*</sup>, and cost, in line with our previous findings).

362 These observations would be consistent with the constant use of antibiotics at low doses that reduces  
363 the optimal PCN. However, similar PCN<sup>\*</sup> values can be achieved by administering higher doses of  
364 antibiotics periodically, as illustrated in [Figure 7B](#) for the case of pBGT. Notice again the non-linear  
365 relationship between PCN<sup>\*</sup> and the frequency of antibiotic exposure. At very low frequencies, the PB  
366 population goes extinct before the first antibiotic pulse and intermediate PCNs maximize the AUC as  
367 in [Figure 4D](#). At high antibiotic frequencies, the PB population persists and oscillates around some  
368 value that increases with PCN. This is consistent with a previous experimental study that evaluated the  
369 stability of costly plasmids in terms of the frequency of environmental fluctuation.<sup>32</sup>

370 Periodic environments provided us with insights into how selection acts on the mean PCN of the  
371 population, but natural environments are not periodic but randomly alternate between intervals of  
372 positive and negative selection. The role of environmental stochasticity in the stability of multicopy  
373 plasmids<sup>23,33</sup> and, in general, in the population dynamics of asexual populations has been widely  
374 studied.<sup>34,35</sup> In our model, we generated stochastic environments that randomly switch from antibiotic-  
375 free to antibiotic for a period of 1,000 days. Each random environment is represented by a sequence  
376 of 1s and 0s, corresponding to days with and without antibiotics, respectively. Therefore stochastic  
377 environments can be characterized by their Shannon's entropy (environmental entropy, H) and the  
378 fraction of days with drug exposure (antibiotic rate, AR) (see [Appendix C](#)). Environments were  
379 classified into "High" and "Low" depending on whether the AR was greater or lower than 0.5. Mind  
380 that each value of H corresponds to two AR values  $AR$  and  $1 - AR$ .

381 Panels on [Figures 7D-E](#) show the PCN\* found by applying the stochastic environments ordered by  
382 entropy (or by AR), for different values of  $\alpha$ . For low values of  $\alpha$ , only high antibiotic rates lead to  
383 plasmid persistence. Notice the non-linear relationship between PCN\* and AR, similar to the observed  
384 for the period in the deterministic setting; PCN\* decreases with AR at low values (corresponding to  
385 extinction) but increases with AR at high values (corresponding to persistence). For higher values of  $\alpha$ ,  
386 we observed that high AR always leads to persistence, while low AR can lead to extinction if entropy is  
387 low. In fact, these low values of the entropy corresponded to long periods without antibiotics that drove  
388 the PB population to extinction. Another interesting remark is that the distribution of obtained PCN\*s  
389 is multi-modal; at fixed entropy, plasmid persistence is achieved by high values of AR that correspond  
390 to high PCN\*, or by low values of AR that correspond to a small value of PCN\*. Similarly, a fixed  
391 value of  $\alpha$  corresponds to two values of PCN\* depending on the antibiotic rate ([Figure 7C](#)).



392  
 393 **Figure 7. Optimal PCNs in fluctuating environments.** **A)** Optimal plasmid copy number (PCN\*) as the  
 394 number of copies that maximizes the area under the curve of Figure 4B. PCN\* decreases exponentially as we  
 395 increase the fitness cost associated with carrying plasmids, as indicated in black-solid line. Black dots show  
 396 some PCN-costs data obtained from the literature. Red dots indicate the values of pBGT. Blue-scale lines  
 397 indicate optimal PCN curves for many values of  $\alpha$ . Light-blues indicate higher values of  $\alpha$  whereas dark-blues  
 398 indicate lower values of  $\alpha$ . Gray line shows the max PCN for the corresponding plasmid cost. **B)** Optimal PCN  
 399 in periodic environments. Each curve corresponds to a value of  $\alpha$ . Black line shows  $\alpha = 0$ . Observe that for very  
 400 short periods optimal PCNs are high, then for certain period the optimal PCN reaches a minimum then as period  
 401 increases, the optimal PCN tends to the optimal of  $\alpha = 0$ . **C-E)** Optimal PCNs using random environments. **C)**  
 402 Environments are classified by their rate of days with antibiotics, the rate differences produce a multi-modal  
 403 outcome, where higher rates increases the optimal PCN and vice-versa. Simulations using the same  
 404 environments were made for different  $\alpha$ s. Note that  $\alpha$  intensity increases the separation of the modes. Modes are  
 405 also classified by their stability, persistence marked with a solid border line and extinction with a dashed border  
 406 line. **D)** Panel of optimal PCNs plotted by the environment entropy for sample  $\alpha$ . Environments are classified by  
 407 their antibiotic rate. **E)** Panel of optimal PCNs plotted by the environment antibiotic rate for sample  $\alpha$ .  
 408 Environments are classified by their entropy.

### 410 **3 Discussion**

411 In this work, we used a population genetics modeling approach to study how non-transmissible  
412 plasmids are maintained in bacterial populations exposed to different selection regimes. In particular,  
413 we considered a small multicopy plasmid that lacks an active partitioning mechanism and therefore  
414 segregates randomly upon cell division. Multicopy plasmids are prevalent in clinical bacteria and usually  
415 carry antimicrobial resistance genes that can be transferred between neighboring bacterial cells,<sup>36</sup> as  
416 well as other evolutionary benefits that go well beyond horizontal transfer.<sup>37</sup> For instance, as multicopy  
417 plasmids are present in numerous copies per cell, the mutational supply increases proportionately  
418 and, once a beneficial mutation appears, its frequency can be amplified during plasmid replication.  
419 This results in an accelerated rate of adaptation to adverse environmental conditions<sup>7</sup> and enables  
420 evolutionary rescue.<sup>38</sup> Also, multicopy plasmids increase the genetic diversity of the population, thus  
421 enhancing survival in fluctuating environments<sup>25</sup> and allowing bacterial populations to circumvent  
422 evolutionary trade-offs.<sup>23</sup>

423 While the benefits of carrying plasmids may be clear under certain circumstances, their maintenance  
424 can be associated with a considerable energetic cost in the absence of selection for plasmid-encoded  
425 genes. This trade-off between segregational stability and fitness cost has been shown to drive ecological  
426 and evolutionary dynamics in plasmid-bearing populations,<sup>39</sup> resulting from multi-level selection acting  
427 on extrachromosomal genetic elements.<sup>40,41</sup> Plasmid population dynamics resulting from random  
428 segregation and replication result in a complex interaction between plasmid copy number, genetic  
429 dominance, and segregational drift, with important consequences in the fixation probability of beneficial  
430 mutations<sup>42</sup> and the repertoire of genes that can be carried in mobile genetic elements.<sup>43</sup> Besides a  
431 reduction in segregational instability, increasing the number of plasmids each cell carries also results  
432 in an increase in gene dosage<sup>44,45</sup> and expression variability of plasmid-encoded genes.<sup>25,46</sup> For  
433 this reason, plasmid control in wild-type bacteria is a tightly regulated process<sup>47</sup> that depends on the  
434 environment and the host's genetics.<sup>8</sup> Precise PCN control is also an important feature of synthetic  
435 genetic circuits that use plasmids as vectors for the production of recombinant substances.<sup>48</sup>

To explore the interaction between the strength of selection and PCN, in this manuscript we postulated discrete-time and Wright-Fisher diffusion models with the following biological assumptions: 1) Plasmids encode for accessory genes that confer an advantage in harsh environments, for instance, antibiotic resistance genes; 2) Bearing plasmids is associated with a fitness cost in the absence of selection for plasmid-encoded genes; 3) Each plasmid segregates randomly to a daughter cell upon division; thus, plasmid bearing bacteria can produce plasmid-free cells with a probability of  $1/2^n$ , where  $n$  is the PCN; 4) The cost associated with plasmid-bearing is constant in time (no compensatory adaptation). We parameterized the model using a well-characterized multicopy plasmid, pBGT,<sup>22–24</sup> and estimated the maximal growth rates of plasmid-bearing and plasmid-free cells by analyzing growth

441  
442  
443  
444  
445  
446  
447  
448  
449  
450  
451  
452  
453  
454  
455  
456  
457  
458  
459  
460  
461  
462  
463  
464  
465  
466  
467  
468  
469  
470  
471  
472  
473  
474

kinetics of each strain grown in isolation. From the growth curves, we obtained estimates for the fitness cost associated with plasmid bearing and the fitness advantage of the plasmid-bearing cells for a range of antibiotic concentrations. We also performed one-day competition experiments between different subpopulations of PB and PF cells and evaluated how this fraction changed after a day of growth in media supplemented with antibiotics. Using this approach we obtained theoretical and experimental iterative maps that we used to predict the long-term dynamics of the system.

Altogether, our results suggest that plasmid population dynamics in bacterial populations is predominantly driven by the existence of a trade-off between segregational loss and plasmid cost. We found that selection is necessary for the persistence of costly plasmids in the long term, and that the strength of selection is highly correlated with the final fraction of plasmids in the entire population. As a result, whether plasmids are maintained or lost in the long term results from the complex interplay between PCN and its fitness cost, as well as the intensity and frequency of positive selection. As shown in the exhaustive exploration of parameters performed in this study, these relationships are highly non-linear, thus resulting in the existence of an optimal PCN that depends on the rate of environmental fluctuation, the number of plasmids carried in each cell, and the fitness burden conferred by each plasmid-encoded gene in the absence of selection. In random environments, we observed a bimodal PCN\* distribution, similar to the plasmid size distribution described for non-transmissible plasmids<sup>49</sup> and for conjugative plasmids.<sup>50</sup>

Although both our theoretical and experimental models consider a multicopy plasmid with random segregation, the existence of an optimal PCN should also hold for non-random segregation (e.g. active partitioning), as this would decrease the probability of segregational loss (which corresponds to having a smaller value of  $\mu_n$  in our model) so its optimal copy number will likely be lower than a plasmid that relies on random segregation.<sup>51</sup> In contrast, compensatory adaptation that reduces the fitness cost associated with plasmid bearing (in our model, a lower value of  $\kappa_n$ ), would result in an increase in PCN\*. We conclude by arguing that, as the existence of plasmids in natural environments requires intermittent periods of positive selection, the presence of plasmids contains information on the environment in which a population has evolved. Indeed, the plasmid copy number associates the frequency of selection with the energetic costs of plasmid maintenance. That is, there is a minimum frequency of drug exposure that allows multiple copies to persist in the population, and, for each environmental regime, there is an optimal number of plasmid copies.

## 475 **References**

- 476 **1.** Chen, J. *et al.* Genome hypermobility by lateral transduction. *Science* **362**, 207–212 (2018).
- 477 **2.** Chen, I. & Dubnau, D. Dna uptake during bacterial transformation. *Nature Reviews Microbiology*  
478 **2**, 241–249 (2004).
- 479 **3.** Funnell, B. E. & Phillips, G. *Plasmid biology*, vol. 672 (ASM press Washington, DC, 2004).
- 480 **4.** Groisman, E. A. & Ochman, H. Pathogenicity islands: bacterial evolution in quantum leaps. *Cell*  
481 **87**, 791–794 (1996).
- 482 **5.** Alonso, J. C. & Tolmasky, M. E. *Plasmids: biology and impact in biotechnology and discovery*  
483 (John Wiley & Sons, 2020).
- 484 **6.** Pemberton, J. & Don, R. Bacterial plasmids of agricultural and environmental importance.  
485 *Agriculture and Environment* **6**, 23–32 (1981).
- 486 **7.** San Millan, A. Evolution of plasmid-mediated antibiotic resistance in the clinical context. *Trends*  
487 *in microbiology* **26**, 978–985 (2018).
- 488 **8.** Alonso-del Valle, A. *et al.* Variability of plasmid fitness effects contributes to plasmid persistence  
489 in bacterial communities. *Nature communications* **12**, 1–14 (2021).
- 490 **9.** Baltrus, D. A. Exploring the costs of horizontal gene transfer. *Trends in ecology & evolution* **28**,  
491 489–495 (2013).
- 492 **10.** San Millan, A. & Maclean, R. C. Fitness costs of plasmids: a limit to plasmid transmission.  
493 *Microbiology spectrum* **5** (2017).
- 494 **11.** Vogwill, T. & MacLean, R. C. The genetic basis of the fitness costs of antimicrobial resistance: a  
495 meta-analysis approach. *Evolutionary applications* **8**, 284–295 (2015).
- 496 **12.** Stewart, F. M. & Levin, B. R. The population biology of bacterial plasmids: a priori conditions for  
497 the existence of conjugationally transmitted factors. *Genetics* **87**, 209–228 (1977).
- 498 **13.** Bergstrom, C. T., Lipsitch, M. & Levin, B. R. Natural selection, infectious transfer and the  
499 existence conditions for bacterial plasmids. *Genetics* **155**, 1505–1519 (2000).
- 500 **14.** Mochizuki, A., Yahara, K., Kobayashi, I. & Iwasa, Y. Genetic addiction: selfish gene's strategy for  
501 symbiosis in the genome. *Genetics* **172**, 1309–1323 (2006).
- 502 **15.** Salje, J. Plasmid segregation: how to survive as an extra piece of dna. *Critical reviews in*  
503 *biochemistry and molecular biology* **45**, 296–317 (2010).
- 504 **16.** Hall, J. P., Wood, A. J., Harrison, E. & Brockhurst, M. A. Source–sink plasmid transfer dynamics  
505 maintain gene mobility in soil bacterial communities. *Proceedings of the National Academy of*  
506 *Sciences* **113**, 8260–8265 (2016).

- 507 **17.** Harrison, E., Koufopanou, V., Burt, A. & Maclean, R. The cost of copy number in a selfish genetic  
508 element: the 2- $\mu$ m plasmid of *Saccharomyces cerevisiae*. *Journal of evolutionary biology* **25**,  
509 2348–2356 (2012).
- 510 **18.** Salverda, M. L., De Visser, J. A. G. & Barlow, M. Natural evolution of *tem-1*  $\beta$ -lactamase:  
511 experimental reconstruction and clinical relevance. *FEMS microbiology reviews* **34**, 1015–1036  
512 (2010).
- 513 **19.** González Casanova, A., Kurt, N., Wakolbinger, A. & Yuan, L. An individual-based model for  
514 the Lenski experiment, and the deceleration of the relative fitness. *Stochastic Processes and their*  
515 *Applications* **126**, 2211–2252 (2016).
- 516 **20.** Salje, J. Plasmid segregation: how to survive as an extra piece of dna. *Critical reviews in*  
517 *biochemistry and molecular biology* **45**, 296–317 (2010).
- 518 **21.** Athreya, K. B. & Ney, P. E. *Branching processes*, vol. 1 (Dover Publications, Inc., Mineola, NY,  
519 2004).
- 520 **22.** San Millan, A., Escudero, J. A., Gifford, D. R., Mazel, D. & MacLean, R. C. Multicopy plasmids  
521 potentiate the evolution of antibiotic resistance in bacteria. *Nature ecology & evolution* **1**, 1–8  
522 (2016).
- 523 **23.** Rodríguez-Beltrán, J. *et al.* Multicopy plasmids allow bacteria to escape from fitness trade-offs  
524 during evolutionary innovation. *Nature ecology & evolution* **2**, 873 (2018).
- 525 **24.** Hernandez-Beltrán, J., Rodríguez-Beltrán, J., San Millán, A., Peña-Miller, R. & Fuentes-Hernández,  
526 A. Quantifying plasmid dynamics using single-cell microfluidics and image bioinformatics.  
527 *Plasmid* 102517 (2020).
- 528 **25.** Hernandez-Beltrán, J. *et al.* Antibiotic heteroresistance generated by multi-copy plasmids. *bioRxiv*  
529 (2022).
- 530 **26.** Hall, B. G., Acar, H., Nandipati, A. & Barlow, M. Growth rates made easy. *Molecular biology and*  
531 *evolution* **31**, 232–238 (2014).
- 532 **27.** Dykhuizen, D. E. Experimental studies of natural selection in bacteria. *Annual Review of Ecology*  
533 *and Systematics* 373–398 (1990).
- 534 **28.** Gullberg, E. *et al.* Selection of resistant bacteria at very low antibiotic concentrations. *PLoS*  
535 *pathogens* **7**, e1002158 (2011).
- 536 **29.** Kumar, P., Maschke, H., Friehs, K. & Schügerl, K. Strategies for improving plasmid stability in  
537 genetically modified bacteria in bioreactors. *Trends in biotechnology* **9**, 279–284 (1991).
- 538 **30.** Greenfield, B. K. *et al.* Modeling the emergence of antibiotic resistance in the environment: an an-  
539 alytical solution for the minimum selection concentration. *Antimicrobial agents and chemotherapy*  
540 **62**, e01686–17 (2018).

- 541 **31.** Yurtsev, E. A., Chao, H. X., Datta, M. S., Artemova, T. & Gore, J. Bacterial cheating drives the  
542 population dynamics of cooperative antibiotic resistance plasmids. *Molecular systems biology* **9**,  
543 683 (2013).
- 544 **32.** Stevenson, C., Hall, J. P., Brockhurst, M. A. & Harrison, E. Plasmid stability is enhanced by  
545 higher-frequency pulses of positive selection. *Proceedings of the Royal Society B: Biological*  
546 *Sciences* **285**, 20172497 (2018).
- 547 **33.** Münch, K., Münch, R., Biedendieck, R., Jahn, D. & Müller, J. Evolutionary model for the unequal  
548 segregation of high copy plasmids. *PLOS Computational Biology* **15**, 1–17 (2019).
- 549 **34.** Kussell, E. & Leibler, S. Phenotypic diversity, population growth, and information in fluctuating  
550 environments. *Science* **309**, 2075–2078 (2005).
- 551 **35.** Raj, A. & van Oudenaarden, A. Nature, nurture, or chance: stochastic gene expression and its  
552 consequences. *Cell* 216–26 (2008).
- 553 **36.** Ares-Arroyo, M., Coluzzi, C. & Rocha, E. P. Towards solving the conundrum of plasmid mobility:  
554 networks of functional dependencies shape plasmid transfer. *bioRxiv* (2022).
- 555 **37.** Rodríguez-Beltrán, J., DelaFuente, J., León-Sampedro, R., MacLean, R. C. & San Millán, Á.  
556 Beyond horizontal gene transfer: the role of plasmids in bacterial evolution. *Nature Reviews*  
557 *Microbiology* 1–13 (2021).
- 558 **38.** Santer, M. & Uecker, H. Evolutionary rescue and drug resistance on multicopy plasmids. *Genetics*  
559 **215**, 847–868 (2020).
- 560 **39.** Paulsson, J. & Ehrenberg, M. Trade-off between segregational stability and metabolic burden: a  
561 mathematical model of plasmid *colE1* replication control. *Journal of molecular biology* **279**, 73–88  
562 (1998).
- 563 **40.** Paulsson, J. Multileveled selection on plasmid replication. *Genetics* **161**, 1373–1384 (2002).
- 564 **41.** Garoña, A., Hülter, N. F., Romero Picazo, D. & Dagan, T. Segregational drift constrains the  
565 evolutionary rate of prokaryotic plasmids. *Molecular Biology and Evolution* (2021).
- 566 **42.** Ilhan, J. *et al.* Segregational drift and the interplay between plasmid copy number and evolvability.  
567 *Molecular biology and evolution* **36**, 472–486 (2019).
- 568 **43.** Rodriguez-Beltran, J. *et al.* Genetic dominance governs the evolution and spread of mobile genetic  
569 elements in bacteria. *bioRxiv* 863472 (2019).
- 570 **44.** Dimitriu, T., Matthews, A. C. & Buckling, A. Increased copy number couples the evolution of  
571 plasmid horizontal transmission and plasmid-encoded antibiotic resistance. *Proceedings of the*  
572 *National Academy of Sciences* **118**, e2107818118 (2021).

- 573 **45.** Million-Weaver, S., Alexander, D. L., Allen, J. M. & Camps, M. Quantifying plasmid copy number  
574 to investigate plasmid dosage effects associated with directed protein evolution. In *Microbial*  
575 *Metabolic Engineering*, 33–48 (Springer, 2012).
- 576 **46.** Jahn, M., Vorpahl, C., Hübschmann, T., Harms, H. & Müller, S. Copy number variability of  
577 expression plasmids determined by cell sorting and droplet digital pcr. *Microbial cell factories* **15**,  
578 1–12 (2016).
- 579 **47.** Del Solar, G. & Espinosa, M. Plasmid copy number control: an ever-growing story. *Molecular*  
580 *microbiology* **37**, 492–500 (2000).
- 581 **48.** Rouches, M. V., Xu, Y., Cortes, L. B. G. & Lambert, G. A plasmid system with tunable copy  
582 number. *Nature communications* **13**, 1–12 (2022).
- 583 **49.** Smillie, C., Garcillán-Barcia, M. P., Francia, M. V., Rocha, E. P. & de la Cruz, F. Mobility of  
584 plasmids. *Microbiol. Mol. Biol. Rev.* **74**, 434–452 (2010).
- 585 **50.** Ledda, A. & Ferretti, L. A simple model for the distribution of plasmid lengths. *arXiv preprint*  
586 *arXiv:1411.0297* (2014).
- 587 **51.** Lopez, J., Donia, M. & Wingreen, N. Modeling the ecology of parasitic plasmids. *ISME J.* **15**,  
588 2843–2852 (2021).
- 589 **52.** Chevin, L.-M. On measuring selection in experimental evolution. *Biology letters* **7**, 210–213  
590 (2011).
- 591 **53.** Gerrish, P. & Lenski, R. The fate of competing beneficial mutations in an asexual population.  
592 *Genetica* **102** (1998).
- 593 **54.** Baake, E., Casanova, A. G., Probst, S. & Wakolbinger, A. Modelling and simulating Lenski’s  
594 long-term evolution experiment. *Theoretical population biology* **127**, 58–74 (2019).
- 595 **55.** Etheridge, A. *Some Mathematical Models from Population Genetics: École D’Été de Probabilités*  
596 *de Saint-Flour XXXIX-2009*, vol. 2012 (Springer Science & Business Media, 2011).
- 597 **56.** R Core Team. *R: A Language and Environment for Statistical Computing*. R Foundation for  
598 Statistical Computing, Vienna, Austria (2020). URL <https://www.R-project.org>.
- 599 **57.** Petzoldt, T. *Estimate Growth Rates from Experimental Data* (2019). URL [https://CRAN.](https://CRAN.R-project.org/package=growthrates)  
600 [R-project.org/package=growthrates](https://CRAN.R-project.org/package=growthrates). R package version 0.8.1.
- 601 **58.** Santos-Lopez, A. *et al.* Compensatory evolution facilitates the acquisition of multiple plasmids in  
602 bacteria. *bioRxiv* 187070 (2017).
- 603 **59.** San Millan, A., Heilbron, K. & MacLean, R. C. Positive epistasis between co-infecting plasmids  
604 promotes plasmid survival in bacterial populations. *The ISME journal* **8**, 601–612 (2014).

## 605 **4 Appendix A: Experimental methods**

### 606 **4.1 Bacterial strains and media**

607 The plasmid free strain we used was *E. coli* K12 MG1655 and the plasmid bearing strain was MG/pBGT  
608 carrying the multicopy plasmid pBGT with the  $\beta$ -lactamase *bla*<sub>TEM-1</sub> which confers resistance to  
609 ampicillin and the fluorescent protein GFP under an arabinose inducible promoter. Mean plasmid copy  
610 number in the population is  $PCN = 19.1 \pm 3.8$ .<sup>22</sup> Overnight cultures were grown in flasks with 20 ml of  
611 lysogeny broth (LB) (Sigma L3022) with 0.5 % w/v L-(+)-Arabinose (Sigma A91906) for fluorescence  
612 induction, in a shaker-incubator at 220 RPM at 37 °C. For the plasmid bearing strain, 25 mg/l of  
613 ampicillin (Sigma A0166) were added to eliminate segregant cells. Ampicillin stock solutions were  
614 prepared at 100 mg/ml directly in LB and sterilized by 0.22  $\mu$ m (Millex-GS SLGS033SB) filtering.  
615 Arabinose stock solutions were prepared at 20% w/v in DD water and sterilized by filtration.

### 616 **4.2 Bacterial growth experiments**

617 Growth kinetics measurements of each strain were performed in 96 well plates with 200  $\mu$ l of LB  
618 with 0.5% w/v arabinose without antibiotics, plates were sealed using X-Pierce film (Sigma Z722529),  
619 each well seal film was pierced in the middle with a sterile needle to avoid condensation. Plates were  
620 grown at 37 degC and reading for OD and fluorescence were made every 20 minutes in a fluorescence  
621 microplate reader (BioTek Synergy H1), after 30 seconds linear shaking.

### 622 **4.3 Competition experiments**

623 Competition experiments were performed using 96-well plates with 200  $\mu$ l of LB with 0.5% w/v  
624 arabinose, and respective ampicillin concentrations: 0, 1, 2, 2.5, 3, 3.5, 4, and 6 mg/l was implemented  
625 by plate rows. To construct our inoculation plate, overnight cultures of the plasmid-free strain and the  
626 plasmid bearing strain were adjusted to an OD of 1 (630 nm) using a BioTek ELx808 Absorbance  
627 Microplate Reader diluted with fresh ice cooled LB. Appropriate volumes were mixed to make co-  
628 cultures at fractions 0, 0.1, 0.2, ..., 1 and set column-wise on a 96-well plate (Corning CLS3370).  
629 We then used a 96 pin microplate replicator (Boekel 140500) with flame sterilization before each  
630 inoculation. Four replicates plates were grown in static incubator at 37°C. After 24 hours growth,  
631 plates were read in a fluorescence microplate reader (BioTek Synergy H1) using OD (630 nm) and  
632 eGFP (479,520 nm) after 1 minute of linear shaking.

### 633 **4.4 Plasmid fraction determination**

To calculate the fluorescence intensity, we first subtracted the background signal of LB for fluores-  
cence and OD respectively, then the debackgrounded the fluorescence signal was scaled by dividing  
by the debackgrounded OD. The measurements for our inoculation plate showed a strong linear  
correlation ( $R^2 = 0.995$ ) between co-cultures fractions and fluorescence intensity (Figure 3B). This  
allowed to directly approximate the populations plasmid fractions from the readings of our compe-

639 titation experiments. We normalized the data independently for each antibiotic concentration taking  
 640 the average measurements of the 4 replicates. Plasmid fractions,  $PF$ , were inferred by normalizing  
 641 the mean fluorescence intensity for each well,  $f_i$ , to the interval  $[0,1]$  using the following formula:  
 642  $PF_i = (f_i - f_{min}) / (f_{max} - f_{min})$  where  $f_{max}$  and  $f_{min}$  are the mean fluorescence intensities at fractions 1  
 643 and 0 respectively.

## 644 5 Appendix B: Mathematical model

### 645 5.1 Fixed points of equation (2)

646 Let  $\bar{f} = f \circ g$ . We want to study the fixed points of  $\bar{f}$  and their domains of attraction. It is not hard to  
 647 see that 0 is always fixed point, and once the frequency reaches 0 it stays at 0. In addition, if  $x \neq 0$ ,

$$\begin{aligned} \bar{f}(x) &= \frac{x(1 - \kappa_n)(1 - \mu_n) / (\alpha - \kappa_n)}{(1 - \alpha) / (\alpha - \kappa_n) + x} = x \\ \Leftrightarrow x^2 + \frac{1 - \alpha}{\alpha - \kappa_n} x &= \frac{(1 - \kappa_n)(1 - \mu_n)}{\alpha - \kappa_n} x \\ \Leftrightarrow x &= \frac{(1 - \kappa_n)(1 - \mu_n) - (1 - \alpha)}{\alpha - \kappa_n} = 1 - \mu_n \frac{1 - \kappa_n}{\alpha - \kappa_n}. \end{aligned}$$

651

652 Denote  $x^* := 1 - \mu_n(1 - \kappa_n) / (\alpha - \kappa_n)$ . Since the frequencies are in  $[0, 1]$ , this fixed point only  
 653 exists if  $\alpha > \kappa_n + \mu_n(1 - \kappa_n)$ . As  $n$  increases,  $\mu_n$  decreases exponentially, while  $\kappa_n$  increases only  
 654 linearly, so there is a non linear relationship between  $n$  and the minimum  $\alpha$  required for the existence  
 655 of a second fixed point  $x^*$ .

Let us analyze the stability of  $x^*$ . Let us assume that  $\alpha > \kappa_n + \mu_n(1 - \kappa_n)$ .

$$\begin{aligned} \bar{f}(x) - x &= \frac{x(1 - \kappa_n)(1 - \mu_n) / (\alpha - \kappa_n) - x(1 - \alpha) / (\alpha - \kappa_n) - x^2}{(1 - \alpha) / (\alpha - \kappa_n) + x} > 0 \\ \Leftrightarrow \frac{(1 - \kappa_n)(1 - \mu_n)}{(\alpha - \kappa_n)} - \frac{1 - \alpha}{\alpha - \kappa_n} - x &> 0 \\ \Leftrightarrow x < x^*. \end{aligned}$$

659

660 So, the frequency increases if it is below  $x^*$  and decreases otherwise, meaning that it is a stable fixed  
 661 point. In addition, the domain of attraction is  $(0, 1]$ , meaning that this equilibrium fraction is reached  
 662 for any initial state.

663 To sum up, 0 is always a fixed point. If  $\alpha > \kappa_n + \mu_n(1 - \kappa_n)$  then there is an additional stable fixed  
 664 points  $x^*$ .

## 665 5.2 Choice of the model

666 In this section, we compare two types of mathematical models for the evolution of plasmid-bearing  
667 frequencies, the discrete time model used in this paper (eq (2)) and the Wright-Fisher diffusion.

668 There had been several attempts to adapt the classical theory of Wright Fisher models to this  
669 experimental setting (see for example<sup>52</sup>). A mathematical rigorous way to do this was developed  
670 in.<sup>19</sup> In<sup>53</sup> an heuristic and applicable to data framework was introduced. Recently, in,<sup>54</sup> the two  
671 methodologies had been paired in order to have a rigorous and applicable way to use classic population  
672 genetics to study evolutionary experiments. In this work, days take the role of generations, and as  
673 the number of individuals after each sampling is more or less constant, the assumption of constant  
674 population size becomes reasonable.

675 Let us assume that the mutation rate  $\mu_{N,n} = 2^{-n}$  and the cost  $\kappa_{N,n}$  are parameterized by  $N$ . To see  
676 the accumulated effects of plasmid costs, segregational loss and genetic drift, we need  $\kappa_{N,n}$  and  $\mu_{N,n}$  to  
677 be of order  $1/N$  (see e.g. Chapter 5 in<sup>55</sup>). The first condition is fulfilled if the cost per plasmid is very  
678 low, for example when  $\kappa_{N,n} = \kappa n/N$ . The second one stands if  $n$  is of order  $\log_2(N)$ , which is the case,  
679 for example, if  $n = 20$  and  $N = 10^6$ , or if  $n = 15$  and  $N = 10^5$ . In that case we set  $\mu = N2^{-n}$ . Under  
680 this setting, when time is accelerated by  $N$ , the frequency process of individuals with plasmids can be  
681 approximated by the solution of the stochastic differential equation (SDE)

$$682 \quad dX_t = -\mu X_t dt - \kappa X_t(1 - X_t)dt + \sqrt{X_t(1 - X_t)}dB_t, \quad (5)$$

683 where  $B$  is a standard Brownian motion. This is known as the Wright-Fisher diffusion with mutation  
684 and selection. When antibiotic is added, at times  $\{T, 2T, \dots\}$ , then (5) modifies to

$$685 \quad dX_t = \sum_{j \geq 1} \frac{\alpha X_{jT-}(1 - X_{jT-})}{1 - \alpha(1 - X_{jT-})} \mathbf{1}_{jT \leq t} - \mu X_t dt - \kappa X_t(1 - X_t)dt + \sqrt{X_t(1 - X_t)}dB_t. \quad (6)$$

686 However, in our experimental setting, the cost that we measure ( $\kappa_n \simeq 0.27$ ) is much higher than the  
687 inverse population size, so we are in the regime of strong selection. In other words, for plasmids that  
688 have a very small cost, of the order of  $1/N$ , genetic drift would play an important role, and the above  
689 Wright-Fisher diffusion with mutation, selection and antibiotic peaks (6) would be the most suitable  
690 model. But in our setting, selection (plasmid costs) is so high that genetic drift becomes negligible.  
691 Recall that equation (2) does not need any time rescaling, whereas, in the diffusion (6) time is measured  
692 in units of  $N$  generations. Under strong selection, the frequencies evolve much faster.

## 697 **6 Appendix C: Numerical simulations**

### 698 **6.1 Computer implementation**

699 The model was implemented in Python, using standard scientific computing libraries (Numpy, Mat-  
700 plotLib, and the Decimal library was required to resolve small numbers conflicts). In general, all  
701 simulations started at PB frequency 1 (unless stated otherwise). Numeric simulations were defined  
702 to reach a steady state when values first repeat. In the case of periodic environments, the repetition  
703 must happen at antibiotic peaks days. We considered extinction if the end point of the realization  
704 dropped below a threshold adjusted to the simulations times, the highest being  $1 \times 10^{-7}$  and the lowest  
705  $1 \times 10^{-100}$ .

### 706 **6.2 Random environments**

707 Environmental sequences of size 1000 (days) using a binomial distribution varying the probability of  
708 success. For each environment created we also bit-flipped (so 101... turns into 010...) and two measures  
709 was applied to each resulting environments. First, we used Shannon entropy,  $H(Env) = -\sum_i^n p_i \log_n(p_i)$ ,  
710 with two states,  $n = 2$  (antibiotic or no-antibiotic) and  $p_i$  equal to the probability of finding an state day,  
711 i.e. the fractions of days with antibiotics and without antibiotics. We classified environments by their  $H$   
712 and by the fraction of antibiotic days, as being this an important feature. This two measures are in the  
713  $[0,1]$  interval so we binned the intervals into 20 bins and 1,000 environments were created for each bin.

### 714 **6.3 Model parametrization**

715 Growth kinetics parameters were estimated using the R<sup>56</sup> package growth rates.<sup>57</sup> Exponential phase  
716 duration,  $\sigma$ , was calculated by finding lag phase duration and the time to reach carrying capacity using  
717 the non-linear growth model Baranyi. Maximum growth rates,  $r$  and  $r + \rho_n$ , were estimated using the  
718 Nonparametric smoothing splines method.  $\kappa_n$  value was estimated using equation (1) and the data from  
719 the antibiotic-free competition experiment using a curve fitting algorithm from the SciPy library in  
720 a custom Python script. Respective values of  $\alpha$  were found in the same manner using equation (2)  
721 and fixing  $\kappa_n$ .  $\kappa_n$  was also calculated using the formula in equation 4 with a very similar result. The  
722 parameters are summarized in [Tables 1](#) and [2](#).

Parameter	Measured value	Formula	Estimated value	Description
r	0.435435	NA	NA	plasmid strain growth rate
$\rho$	0.052334	NA	NA	WT growth rate advantage
$\sigma$	6.074089	NA	NA	exponential phase duration
$\mu_n$	NA	$\mu_n = 1 - \frac{r2^{-n} + \rho}{r2^{-n}e^{(r2^{-n} + \rho)\sigma} + \rho}$	5.938e-06	1-day fraction of segregants
$\kappa_n$	NA	$\kappa_n = \frac{\rho(1 - e^{-(r2^{-n} + \rho)\sigma})}{r2^{-n} + \rho}$	0.272313	fitness cost
n	19	NA	NA	plasmid copy number

723 **Table 1.** Model parameters estimated using growth curves experiments in the absence of antibiotics.

Amp	$\kappa_n$	$\alpha$
0.0	0.272276	0.0
1.0	0.272276	-0.37781
2.0	0.272276	-0.332662
2.5	0.272276	-0.058457
3.0	0.272276	0.992911
3.5	0.272276	0.9801
4.0	0.272276	0.992075
6.0	0.272276	0.99373

726 **Table 2.** Model parameter estimated by fitting equation (4) to experimental data obtained for a range  
728 of ampicillin concentrations.

Name	Plasmid Type	Species	PCN	PCN SD	Cost	Cost SD	Reference
pB1006	ColE1	<i>Haemophilus influenzae</i> RdKW20	10.530	1.112	0.021	0.012	58
pB1005	ColE1	<i>Haemophilus influenzae</i> RdKW20	20.450	2.590	0.05	0.013	58
pB1000	ColE1	<i>Haemophilus influenzae</i> RdKW20	25.020	1.920	0.054	0.002	58
pNI105		<i>Pseudomonas aeruginosa</i>	18.000	2.400	0.132	0.025	59
2-uM		<i>Saccharomyces cerevisiae</i>	52.000	0.000	0.0884	0.00416	17
pNUK73		<i>Pseudomonas aeruginosa</i>	11.030	1.890	0.214	0.008	59
pBGT	ColE1	<i>Escherichia coli</i>	19.120	1.560	0.057	0.013	22
pBGT R164S	ColE1	<i>Escherichia coli</i>	21.100	0.850	0.057	0.003	22
pBGT G54U	ColE1	<i>Escherichia coli</i>	44.500	3.810	0.207	0.019	22
pBGT G55U	ColE1	<i>Escherichia coli</i>	88.930	15.650	0.443	0.116	22
pBGT R164S G54U	ColE1	<i>Escherichia coli</i>	52.300	2.190	0.238	0.016	22
pBGT R164S G55U	ColE1	<i>Escherichia coli</i>	127.290	4.580	0.491	0.082	22

730 **Table 3.** Plasmid copy number and plasmid costs from literature. SD Standard Deviation.